REPUBLIQUE ALGERIENNE DEMOCRATIQUE ET POPULAIRE

MINISTERE DE L'ENSEIGNEMENT SUPERIEUR ET DE LA RECHERCHE SCIENTIFIQUE

UNIVERSITE MOHAMED BOUDIAF - M'SILA

FACULTE DE TECHNOLOGIE

DEPARTEMENT D'ELECTRONIQUE

N° :

DOMAINE : SCIENCE ET TECHNOLOGIE

FILIERE : ELECTRONIQUE

OPTION : MICROELECTRONIQUE

MEMOIRE PRESENTE POUR L'OBTENTION
DU DIPLOME DE MASTER ACADEMIQUE

Par:

DAOUDARI MOHAMED

TOURI ALI

Intitulé

SEMI -CONDUCTOR BEHAVIOR SURVEY IN SOME MAGNETIC MATERIALS

Soutenu devant le jury composé de:

HARHOUZ Ahlam	**Université Mohamed Boudiaf M'sila**	**Président**
KETFI Mohamed El-Amin	**Université Mohamed Boudiaf M'sila**	**Rapporteur**
SAAD ESSAOUD Saber	**Université Mohamed Boudiaf M'sila**	**Examinateur**

Le **10/06/2024**

Année universitaire : 2023 / 2024

شكر وعرفان

نشكر الله عز وجل الذي وفقنا لإنجاز هذا العمل المتواضع وامدنا بالهمة والمثابرة والدعم من اجل المواصلة

ونتقدم بجزيل الشكر إلى الاستاذ "كتفي محمد الامين"

الذي اشرف على هذا العمل وما تقدم به لنا من عون وتوجيهات.

كما اتوجه بالشكر الجزيل إلى الأستاذة " حرحوز أحلام " على تفضله برئاسة لجنة المناقشة والأستاذ " ساعد السعود صابر" على قبوله تقييم هذا العمل.

وأخيرا نشكر كل من قدموا لنا يد العون وإلى كل من ساعدنا لإتمام هذا العمل سواء من قريب او من بعيدا ولو بكلمة طيبة أو بدعوة صادقة.

الاهداء

إلى التي حملتني وهنا على وهن وسقتني من نبع حنانها الفياض

إلى من كان دعاؤها ورضاها عني سر نجاحي أمي الغالية حفظها الله

إلى رمز الكفاح في الحياة إلى الذي تعب من اجل تربيتي

إلى من غرس القيم والاخلاق في قلبي

إلى من أحمل لقبه بكل فخر واعتزاز أبي أطال الله في عمره

إلى كل زملائي طيلة مساري الدراسي

إلى من علمني حرفا فصرت له عبدا أساتذتي الكرام من الطور الإبتدائي إلى الجامعة

إلى كل هؤلاء أهدي ثمرة جهدي

محمد

الاهداء

أحمد الله عز وجل على عونه لإتمام هذا البحث.

إلى الذي وهبني كل ما يملك حتى أحقق له آماله، إلى من كان يدفعني قدما نحو الأمام لنيل المبتغى، إلى الإنسان الذي إمتلك الإنسانية بكل قوة أبي الغالي على قلبي أطال الله في عمره .

إلى التي وهبت فلذة كبدها كل العطاء و الحنان، إلى التي صبرت على كل شيء، التي رعتني حق الرعاية و كانت سندي في الشدائد، و كانت دعواها لي بالتوفيق، تتبعتني خطوة خطوة في عملي، إلى من إرتحت كلما تذكرت إبتسامتها في وجهي نبع الحنان أمي شمس حياتي أعز ملاك على القلب و العين جزاها الله عني خير الجزاء في الدارين .

إليهما أهدي هذا العمل المتواضع لكي أُدخل على قلبهما شيئا من السعادة إلى إخوتي أيمن وأشرف و أخواتي شيماء وأمينة الذين تقاسمو ا معي عبء الحياة

كما أهدي ثمرة جهدي لأستاذي الكريم الدكتور: كتفي محمد

الذي كلما تظلمت الطريق أمامي لجأت إليه فأنار ها لي و كلما دب اليأس في نفسي زرع فيا الأمل لأسير قدما و كلما سألت عن معرفة زودني بها و كلما طلبت كمية من و قته الثمين وفره لي بالرغم من مسؤولياته المتعددة

الى من شاركني رحلة هذا البحث صديقي محمد

و إلى كل من يؤمن بأن بذور نجاح التغيير هي في ذواتنا و في أنفسنا قبل أن تكون في أشياء أخرى.

علي

Table of Contents

Chapter 2 : Results and discussion

List of Figures

List of Tables

List of Abbreviations

DFT	Density functional theory
DOS	Density-of-states
FP-LAPW	Full-potential linearized augmented plane wave
GGA	Generalized gradient approximation
HF	Hartree-Fock
KS	Kohn-Sham
PAW	Projector augmented wave
PBE	A simplified GGA
PV	Photovoltaic

General Introduction

General Introduction

With the global shift towards renewable energies gaining momentum, scientific exploration in both experimental and theoretical realms is accelerating toward harnessing solar energy, a vital and inexhaustible resource [1,2]. This involves converting light energy into electrical energy through mechanisms like solar panels and photovoltaic systems. The genesis of solar panel technology traces back to the recognition of the potential for generating electrical energy by exposing certain materials to sunlight. Subsequent research, including the discovery of selenium, significantly propelled advancements in this technological domain, leading to its application in various fields such as computing and satellite technology [3].

The effectiveness of photovoltaic technologies hinges on numerous factors, with material composition playing a pivotal role. Despite its promise, widespread adoption of photovoltaics faces a notable obstacle in its relatively high cost.

Delafossite is a fascinating mineral that has captured the attention of scientists and researchers due to its unique combination of properties. Comprised primarily of copper, aluminum, and oxygen, Delafossite exhibits remarkable electrical conductivity while also maintaining transparency to visible light. This unusual duality of conductivity and transparency makes delafossite materials highly sought after for a range of electronic applications [4]. In nature, Delafossite typically forms as thin platy crystals or in massive form, show casing its hexagonal crystal structure. Its chemical formula, $CuAlO_2$, reflects its composition of copper, aluminum, and oxygen atoms arranged in a specific lattice configuration.

Researchers have been exploring the potential of Delafossite materials in various electronic devices, including solar cells, touchscreens, and light-emitting diodes (LEDs). Their conductivity allows for efficient electrical conduction, while their transparency enables light to pass through unhindered, making them ideal candidates for applications requiring both electrical conductivity and optical transparency [5].

The study of Delafossite minerals continues to yield insights into their properties and potential applications, driving innovation in the field of materials science and electronics. Its structure is characterized by its layered configuration. It crystallizes in a rhombohedral or hexagonal system, with space groups R3m or P63/mmc. The layers consist of linear A-B-X units where A atoms are linearly coordinated with B atoms. The B atoms are typically surrounded by an octahedral coordination of X atoms. The lattice parameters and atomic

positions within the unit cell are critical for determining the stability and properties of the material [6-9].

The optoelectronic properties of Delafossite compounds are pivotal for their application in electronic and photonic devices. These properties include the band gap, electrical conductivity, and optical absorption. The electronic structure, determined by the arrangement and types of A, B, and X atoms, plays a crucial role in their optical transparency and electrical conductivity [10].

The magnetic properties of Delafossite compounds arise from the magnetic moments of the transition metal B atoms. These materials can exhibit various magnetic behaviors such as antiferromagnetism, ferromagnetism, and spin glass states, influenced by the super-exchange interactions between B-site cations mediated by X anions. Understanding the magnetic interactions and anisotropy is essential for potential applications in spintronics where materials are required to have specific magnetic orientations and behaviors [11].

The theoretical investigation of Delafossite compounds involves computational methods such as density functional theory (DFT) to predict and analyze their structural, electronic, and magnetic properties. By employing various exchange-correlation functionals and computational models, researchers can simulate the crystal structure, electronic band structure, density of states (DOS), and magnetic ordering. These theoretical insights are instrumental in guiding experimental synthesis and tailoring the properties of delafossite compounds for specific applications.

The aim of this study is to enhance our comprehension of the structural, electronic, optical and magnetic of Delafossite compound $BrCdO_2$ using the Wien2k calculation software. This research is organized into two chapters, each with a specific goal. The first chapter offers a theoretical foundation for analyzing crystalline systems, drawing upon principles of quantum mechanics. It begins with an exploration of the time independent Schrödinger equation, which describes the behavior of electrons and nuclei within a system. Significant approximations such as the Born-Oppenheimer, Hartree, Hartree-Fock, and Density Functional Theory (DFT) are explained, focusing particularly on their role in estimating exchange-correlation interactions among electrons. Chapter 2 goes into more details calculation of the structural properties by GGA approximations and determined some structural properties as cell constants, compressibility modulus and cohesive energy. The Density Functional Theory (DFT) will be used as the main tools of the study. In the first stage, we will perform a structural phase stability

of different potential phases of $BrCdO_2$. We studied the electronic behavior of the compound, where we determined the value of the energy gap, as well as the electronic orbitals contributing to each energy band by studying the density of state curves, in addition to determining the type of bonds between atoms based on the charge density distribution curves in the interfacial region. As for the optical properties, we studied both the absorption coefficient and the reflection coefficient, the coefficients of inertia and refraction and the energy loss coefficient for the compound, while comparing all the results obtained with what has been obtained in other scientific research, Finally, we summarize the results of our work and give the direction for future works.

References

[1] L. Hong, H. Yao, Z. Wu, Y. Cui, T. Zhang, Y. Xu, R. Yu, Q. Liao, B. Gao, K. Xian, Eco-compatible solvent-processed organic photovoltaic cells with over 16% efficiency, Adv. Mater. 31 (2019) 1903441.

[2] J. Gong, C. Li, M.R. Wasielewski, Advances in solar energy conversion, Chem. Soc. Rev. 48 (2019) 1862–1864.

[3] D. W. LANE, K. J. HUTCHINGS, R. Mc Cracken, New Chalcogenide Materials for Thin Film Solar Cells, The Royal Society of Chemistry (2015) 160-167.

[4] Atuchin, V. V., et al. "Structural and electronic properties of delafossite-type oxides." Journal of Physics and Chemistry of Solids, vol. 69, no. 4, 2008, pp. 967-973.

[5] Cox, P. A. Transition Metal Oxides: An Introduction to Their Electronic Structure and Properties. Clarendon Press, 2010.

[6] Kawazoe, H., et al. "P-type electrical conduction in transparent thin films of CuAlO2." Nature, vol. 389, no. 6654, 1997, pp. 939-942.

[7] Rondinelli, J. M., and Spaldin, N. A. "Structure and properties of functional oxide thin films: Insights from electronic-structure calculations." Advanced Materials, vol. 23, no. 30, 2011, pp. 3363-3381.

8] Singh, D. J., and Mazin, I. I. "Electronic structure and magnetism of delafossite oxides." Physical Review B, vol. 63, no. 16, 2001, p. 165101.

[9] Yanagi, H., et al. "Electronic structure and optoelectronic properties of delafossite-type oxides: CuScO2, CuYO2, and CuLaO2." Journal of Applied Physics, vol. 88, no. 7, 2000, pp. 4159-4163.

[10] Yoshida, H., et al. "Transparent p-type semiconducting CuAlO2 thin films prepared by pulsed laser deposition." Applied Physics Letters, vol. 80, no. 5, 2002, pp. 802-804.

[11] Zhang, J., et al. "High-throughput computational search for transparent conducting oxides." Journal of Materials Chemistry C, vol. 4, no. 6, 2016, pp. 1430-1440.

[9] Yanagi, H., et al. "Electronic structure and optoelectronic properties of delafossite-type oxides: CuScO2, CuYO2, and CuLaO2." Journal of Applied Physics, vol. 88, no. 7, 2000, pp. 4159-4163.

[10] Yoshida, H., et al. "Transparent p-type semiconducting CuAlO2 thin films prepared by pulsed laser deposition." Applied Physics Letters, vol. 80, no. 5, 2002, pp. 802-804.

[11] Zhang, J., et al. "High-throughput computational search for transparent conducting oxides." Journal of Materials Chemistry C, vol. 4, no. 6, 2016, pp. 1430-1440.

CHAPTER 1

CHAPTER 1:

THEORETICAL STUDY OF MANY-PARTICLES SYSTEM

Table of Contents

1. The Schrödinger equation

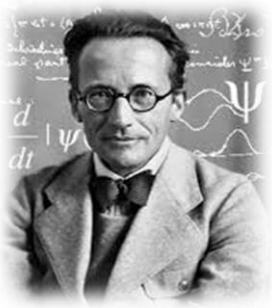

In 1926, the physicist Erwin Schrödinger proposed a partial differential equation known as the Schrödinger equation in the framework of quantum theory [1]. The solution of this equation allows us to describe the instantaneous quantum state of a system through its wave function, which includes all the information about the system studied [2–4]. The Schrödinger equation has the following expression:

$$H\Psi(\vec{R}_I, \vec{r}_i) = E\Psi(\vec{R}_I, \vec{r}_i) \qquad \textbf{(I.1)}$$

The two vectors $\vec{R}_I$ and $\vec{r}_i$ are the coordinates of the nucleus (I) and of the electron (i).

H: Hamiltonian operator related to the sum of the kinetic energy and the potential energy of the system.

E: Energy eigenvalue of the system.

Ψ: Wave function which depends on the coordinates of electrons and nuclei.

The Hamiltonian system - made up of nuclei and electrons - includes the kinetic energy of electrons and nuclei, as well as the potential energies (electron-electron, electron-nucleus, and nucleus-nucleus), therefore the expression of the total Hamiltonian of the system is written by the following expression:

$$H = Te + TN + Vee + Ve{-}N + VN{-}N \qquad \textbf{(I.2)}$$

$T_e = -\sum_i \frac{\hbar^2}{2m_i}\vec{\nabla}_i^2 \rightarrow$ Electronic kinetic energy (m_i the mass of electron i).

$T_n = -\sum_I \frac{\hbar^2}{2m_I}\vec{\nabla}_I^2 \rightarrow$ Nuclei kinetic energy (m_I the mass of the nucleus I).

$V_{N-N} = \sum_{I\neq J} \frac{Z_I Z_J e^2}{|R_I - R_J|} \rightarrow$ The interaction part between the nuclei.

$V_{e-N} = \sum_{I,j} \frac{Z_I e^2}{|R_I - r_j|} \rightarrow$ The nuclei-electrons interaction part.

$V_{e-e} = \sum_{i\neq j} \frac{e^2}{|r_i - r_j|} \rightarrow$ The interaction part between the electrons.

$|R_\alpha - R_\beta|$ → The distance between the two nuclei α and β

$|r_i - R_\alpha|$ → The distance between the nucleus α and the electron i

$|r_i - r_j|$ → The distance between the two electrons i and j.

In practice, the Schrödinger equation is difficult to solve and the exact solution cannot be obtained, especially for systems containing large numbers of electrons and nuclei in motion and interaction between them, so simplifications and approximations must be used to obtain an approximate solution that is as close to the real solution as possible. The following are some of the most notable approximations and simplifications to the Schrödinger equation:

2. Born-Oppenheimer approximation

The Born-Oppenheimer approximation [5], developed in 1927 by physicists Max Born and Robert Oppenheimer, allowed to separate the movement of nuclei from the movement of electrons. Despite its movement, the nucleus remains very close to its equilibrium with respect to the electrons, which are very fast, and thus it is possible to ignore the nuclei's kinetic energy in regards to the electrons' kinetic energy and consider the nucleus-nucleus interaction energy as a constant quantity (V_{nn} = Constant).

According to the Born-Oppenheimer approximation we can rewrite the total wave function of the system $\Psi\left(\vec{R}_I^{\,0},\vec{r}_i\right)$ in the form of a product of an electronic function $\Psi_e\left(\vec{R}_I^{\,0},\vec{r}_i\right)$ and a nuclear function $\Psi_n\left(\vec{R}_I^{\,0}\right)$, thus, we can separate the motion of nuclei from that of electrons. Then the wave function is written:

Despite applying this simplification to the Schrödinger equation, the problem remains difficult and cannot be solved using current mathematical methods due to the extremely complicated electron-electron interaction, thus we used additional approximations.

$$\Psi\left(\vec{R}_I^{\,0},\vec{r}_i\right) = \Psi_n\left(\vec{R}_I^{\,0}\right)\Psi_e\left(\vec{R}_I^{\,0},\vec{r}_i\right)$$

$$\begin{cases} [T_e + V_{ee} + V_{en}]\Psi_e\left(\vec{R}_{\mathrm{I}}^{\,0},\vec{r}_{\mathrm{i}}\right) = E_e\left(\vec{R}_{\mathrm{I}}^{\,0}\right)\Psi_e\left(\vec{R}_{\mathrm{I}}^{\,0},\vec{r}_{\mathrm{i}}\right) \\ \left[T_n + V_{nn} + E_e\left(\vec{R}_{\mathrm{I}}^{\,0}\right)\right]\Psi_n\left(\vec{R}_{\mathrm{I}}^{\,0}\right) = E\Psi_n\left(\vec{R}_{\mathrm{I}}^{\,0}\right) \end{cases}$$

3. Hartree and Hartree-Fock approximations (HF)

The Hartree-Fock approximation was proposed to modify and correct the shortcomings of the Hartree approximation. Hartree proposed in 1928 [6,7] that all electrons be treated as identical particles that move independently without interacting with other particles (independent particle approximation [8]). In this approximation, Hartree treats the interactions between electrons as particles carrying a charge without taking into account the spin state, i.e. the interactions that occur between them are Columbian repulsion interactions with neglecting both exchange and correlation terms. Furthermore, the wave function is not "antisymmetric" since it does not take into consideration the Pauli exclusion principle [3,4].

Although the Hartree approximation does not take in account the electron spin and the Pauli exclusion principle, it simplifies the Schrödinger equation from studying a large number of electrons to studying a single electron, so that the total Hamiltonian H of electrons is the sum of the Hamiltonians h_i of each electron, while the total wave function of the electronic system represents by multiplication the individual wave functions of each electron [3,4]. Finally, the total energy of the electronic system is the sum of the energies of all electron. According to Hartree's approximation, the Hamiltonian equation for single electron can be written as follows:

$$H = \sum_i h_i \tag{I.3}$$

$$h_i = -\frac{\hbar^2}{2m_i}\Delta_i - \sum_I \frac{Z_I e^2}{\left|\vec{r_i} - \vec{R_I}^0\right|} + \frac{1}{2}\sum_j \frac{e^2}{\left|\vec{r_i} - \vec{r_j}\right|}$$

$$\Psi_e = \prod_i \Psi_i \tag{I.4}$$

$$E_e = \sum_i \varepsilon_i \tag{I.5}$$

In 1930, Fock [9] improved and modified Hartree's model by substituting the wave functions of the electron with a Slater determinant[10], allowing him to accommodate for the exchange effect that Hartree neglected. In this way, the interaction between electrons takes into account both the coulomb interaction and the exchange effect, and thus the previous functions have been replaced by anti-symmetric functions, and therefore, Fock introduced the term spin in its dealing with electronic interactions and replaced the wave function of the electronic system by a Slater determinant expressed by the formula:

$$\Psi_{HF}(\vec{r}_1, \vec{r}_2, \vec{r}_3, \dots, \vec{r}_N) = \frac{1}{\sqrt{N_e!}} \begin{bmatrix} \psi_1(\vec{r}_1) & \psi_1(\vec{r}_2) & \psi_1(\vec{r}_3) & \cdots & \psi_1(\vec{r}_N) \\ \psi_2(\vec{r}_1) & \psi_2(\vec{r}_2) & \psi_2(\vec{r}_3) & \cdots & \psi_2(\vec{r}_N) \\ \psi_3(\vec{r}_1) & \psi_3(\vec{r}_2) & \psi_3(\vec{r}_3) & \dots & \psi_3(\vec{r}_N) \\ \vdots & \vdots & \vdots & \ddots & \vdots \\ \psi_N(\vec{r}_1) & \psi_N(\vec{r}_2) & \psi_N(\vec{r}_3) & \cdots & \psi_N(\vec{r}_N) \end{bmatrix} \tag{I.6}$$

$\frac{1}{\sqrt{N_{e!}}}$ Where is a normalization factor.

4. Density Functional Theory (DFT)

The aim behind Density Functional Theory (DFT) is to rewrite the Hamiltonian of the electron using electron density rather than wave functions. Researchers like Dirac [11], Slater [12], Hohenburg, and Kohn [13] have made significant contributions to this theory through their theoretical work.

The DFT theory was first discovered in the works of Thomas and Fermi in 1927[13,4], where they created the main idea in expressing the total energy of an electronic system as a

function of electron density by considering the electronic system as a homogeneous and regular gas of electrons where the continuous partitioning of the Brillouin zone (without taking into consideration electron correlations) was carried out by the two scientists Thomas and Fermi in order to achieve regions where the electron density is constant in each part. The following two formulas provide expressions for the density and kinetic energy of a homogeneous electronic gas:

$$\rho = \frac{1}{3\pi^2} E_f^{\frac{3}{2}} \left(\frac{2m_e}{h^2}\right)^{\frac{3}{2}} \quad \textbf{(I.7)}$$

$$E_c = \frac{3}{5}\left(\frac{h^2}{2m_e}\right)(3\pi^2)^{\frac{2}{3}}\rho^{\frac{5}{2}} \quad \textbf{(I.8)}$$

The following table presents a comparison between Hartree-Fock method and density functional theory and the characteristics of each method [3].

Table I. 1: Comparison between the two methods, Hartree-Fock and the Density Functional Theory (DFT) [16,17]

HF method	DFT
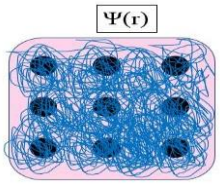	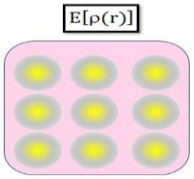
• Principle: Solving the Schrödinger equation by considering the wave functions as a variable basic. Based on the mean field theory (MFT). • Calculates wave functions and eigenvalue energy to obtain ground state energy. • Depend on the large number of variables, which makes the equation very complicated and time consuming. • The wave functions obtained as solutions for the Schrödinger equation have no physical meaning. Does not take into • account the correlation terms.	• Principle: Solving the Schrödinger equation by considering the electron density as a variable basic. • Based on the two Hohenburg – Sham theorems and shifting from the Schrödinger equation to the KohnSham equations to find the solution. • Use electron density which has physical meaning. • Reduce the number of variables which makes the equation simpler and faster compared to the HF method. • Enable to treat the correlation terms.

4.1. Formalism of density functional theory (DFT)

The density functional theory (DFT) is based on describing the total energy of a system with many interacting electrons as a function of the electronic density, rather than its wave function, where the electronic density is expressed by the formula:

$$\rho(\vec{r}) = \sum_{i=1}^{N} |\Psi_i(\vec{r})|^2 \qquad \textbf{(I.9)}$$

The density functional theory (DFT) is based on two main theorems.

I. The theorems of Hohenburg and Kohn

The two theorems presented by Hohenburg and Kohn in 1964, are considered to be the basis of the density functional theory.

A-1) First theorem:

The total energy of an electronic system is a functional of the electron density for an external potential V (r), so it is possible to know all the properties of the system when determining the electron density[3,18].

$$[(r)] = [(r)] + \int V(r)(r)dr^3 \qquad \textbf{(I.10)}$$

Where F [ρ] is universal functional.

The external potential and the universal functional F [ρ] are expressed in the form:

$$V_{ext}(\vec{r_i}) = -\sum_A \frac{Z_A}{r_{iA}} \qquad \textbf{(I.11)}$$

$$[\rho] = [\rho] + U[\rho] \qquad \textbf{(I.12)}$$

Where Z_A is the charge of the nucleus, r_{iA} is the distance between nucleus A and electron i.

A-2) Second theorem:

The second theory appears that to obtain the total energy of the ground state of the electronic system, it is enough to find the corresponding electron density which makes the density function at its minimum value.

$$E\left(\rho_0(\vec{r})\right) \leq E[\rho(\vec{r})]$$

$$E(\rho_0) = MinE(\rho) \lim_{\rho \to N} \langle \Psi | \hat{T} + \sum_i V_{ext} + V_{ee} | \Psi \rangle \quad \textbf{(I.13)}$$

We can get the corresponding electron density of the ground state, by applying the variational principle via the differential of total energy in terms of electron density:

$$\frac{dF[\rho(r)]}{d\rho(r)} + V(r) = 0 \quad \textbf{(I.14)}$$

Therefore, if the electron density which minimizes the energy function is known, we can easily determine the wave function and the exact energy of the ground state.

II. The Kohn - Sham equation

One of the difficulties in studying a manyelectrons system is the inability to express the kinetic energy and electron-electron interactions analytically in terms of electron density.

In 1965, scientists Kohn and Sham suggested the initial idea of replacing the real electronic system with a fictive system in which the behavior of the electron is independent, unrelated, and unaffected by the behavior of other electrons. It is only affected by the effective potential (Kohn-Sham potential), which involves both the external potential created by the nuclei's influence and the potential caused by the remaining particles effect on this electron[3,19,20].

The fictive system proposed by Kohn-Sham is characterized by:

- ✓ The Kohn-Sham orbits which are space wave functions of a single electron are solutions of the Schrödinger equation in this vacuum space.
- ✓ The fictive electronic system has the same electronic density as a real system.
- ✓ The kinetic energy of the fictive system is the kinetic energy of the electrons without the correlation effect and it is positive, while the kinetic energy in the real system "T_R" is the sum of the kinetic energy of the fictive system "Tf" and an additional term that expresses the effect of the correlation "Tc" on the kinetic energy of the electron [3] that is:

$$T_R = T_f + T_c \qquad \textbf{(I.15)}$$

$$T_c = \langle \Psi | T | \Psi \rangle - \langle \varphi | T_s | \varphi \rangle \qquad \textbf{(I.16)}$$

The V_{ee} interaction between electrons in the real system which is written in the following relation:

$$\langle \Psi | V_{ee} | \Psi \rangle = U_H + U_x + U_c \qquad \textbf{(I.17)}$$

Where the terms represent:

U_H: The electron-electron coulomb interaction (Hartree potential)

U_x: The exchange energy between electrons of the same spin.

Uc: The correlation energy between the electrons.

The Kohn-Sham equation for an electronic system is given as a function of the kinetic energy of the electron: external potential energy, Hartree interaction and exchange-correlation energy as follows:

- ✓ The kinetic energy of an electron in a fictitious system:

$$T_s[\rho] = \left\langle \varphi_i \left| -\frac{\hbar^2}{2\mathrm{m}} \Delta \right| \varphi_i \right\rangle = -\frac{\hbar^2}{2\mathrm{m}} \sum_{\mathrm{i}} \int \varphi_i \nabla^2 \varphi_i^* dr_i \qquad \textbf{(I.18)}$$

- ✓ The external potential generated by the effect of nuclei (nucleus-electron interaction):

$$V_{NE}[\rho] = -\int \sum_{I,i} \frac{Z_I \rho(\vec{r})}{\left|\vec{R}_I^{\,0} - \vec{r}\right|} dr \qquad \textbf{(I.19)}$$

- ✓ The Hartree potential (electron-electron coulomb interaction)

$$U[\rho] = \frac{1}{2}\int \frac{\rho(\vec{r})\rho(\vec{r'})}{\left|\vec{r} - \vec{r'}\right|} dr dr' \qquad \textbf{(I.20)}$$

- ✓ The exchange-correlation energy, which is the sum of the correlation and exchange terms, it does not have an exact mathematical expression, but it is estimated by approximations

$$E[\rho] = E_x[\rho] + E_c[\rho] \qquad \textbf{(I.21)}$$

And finally, the Kohn-Sham equation is written as follows [21–23]:

$$H_{KS}\varphi_i(r) = [T_s[\rho] + V_{KS}(r)]\varphi_i(r) = \varepsilon^{KS}\varphi_i(r) \qquad \textbf{(I.22)}$$

$$V(r) = V_{ext}(r) + V_H(r) + + V_{XC}(r) \qquad \textbf{(I.23)}$$

$$[\rho] = T[\rho] + V_{NE}[\rho] + U_H[\rho] + E_{xc}[\rho] \qquad \textbf{(I.24)}$$

B-1) Solution of the Kohn - Sham equation

Solving the Kohn-Sham equation depends on two basic steps:

- The first step: define all the terms of the effective Kohn-Sham potential, i.e. the exchangecorrelation potential E_{xc} must be determined because this term has no mathematical formula but it can be estimated by approximations.

- The second step: find the wave functions (Kohn-Sham orbits), which represent a solutions for the Kohn-Sham equation given by [3]:

$$\varphi(r) = \sum_j C_{ij}\,\varphi_j(r) \qquad \textbf{(I.25)}$$

Where (r) are the basic functions, and Cij are are the development coefficients.

$$\sum_j Cij\ HKS|\varphi j\rangle = \sum_j Cij\varepsilon KS\ |\varphi j\rangle \qquad \textbf{(I.26)}$$

$$\langle\varphi k|\sum_j Cij\ HKS|\varphi j\rangle = \langle\varphi k|\sum_j Cij\varepsilon KS\ |\varphi j\rangle \qquad \textbf{(I.27)}$$

$$\sum_j \left(\langle\varphi_k|H_{KS}|\varphi_j\rangle - \varepsilon_{KS}\langle\varphi_k|\varphi_j\rangle\right)_j = 0 \qquad \textbf{(I.28)}$$

It remains to determine the C_{ij} coefficients.

The Kohn-Sham equation is solved according to an iterative cycles illustrated by figure (1.I), where the process starts using an initial density $\rho_{in}$for the first iteration, this density is used to solve the Kohn-Sham equation, then, We use a superposition of the atomic densities and we compute the Kohn-Sham matrix, to solve the equations, then obtain the Kohn-Sham orbitals.

After this step, we calculate the new densityρ_{out}, to check the convergence condition (if the density or energy has changed a lot or not) and we mixed the two charge densities $\rho_{out}$and ρ_{in}as follow:

$$\rho_{in}^{i+1} = (1-\alpha)\rho_{in}^{i} + \rho_{out}^{i} \qquad \textbf{(I.29)}$$

Thus the iterative procedure can be repeated until the convergence condition is fulfilled.

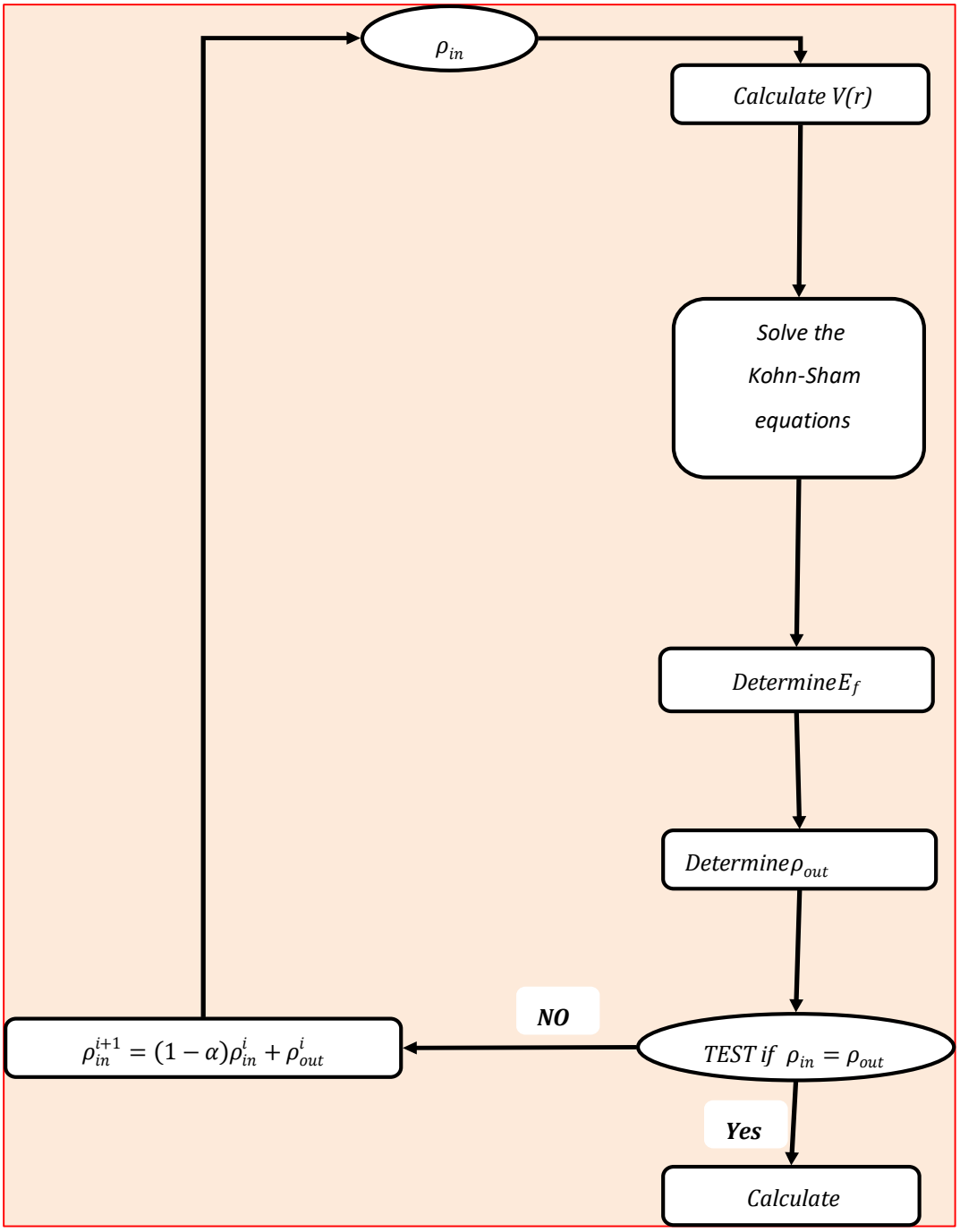

Figure I. 1: Self-consistent calculation.

5. The different types of approximations of the $E_{XC}[\rho]$

As the exchange-correlation potential between electrons has no analytical term, several scenarios have been used to obtain approximate values for this potential, the accuracy of the results obtained being mainly related to the mathematical formula of this potential[3].

5.1. Local density approximation (LSDA)

This model was first proposed by Kohn and Sham in 1964 [24] where the inhomogeneous electronic system is approximated by a local homogeneous electronic system after dividing the Brillouin region into small regions, and the expression energy exchange - correlation is given by the relation :

$$E_{XC}^{LSDA} = \int \rho(\vec{r})\, E_{xc}[\rho(\vec{r})] d\vec{r}$$

$$V_{xc} = \frac{dE_{XC}^{LDA}[\rho]}{d\rho} = \varepsilon_{XC}^{LDA} + \rho(\vec{r})\frac{d\varepsilon_{XC}^{LDA}}{d\rho} \qquad \textbf{(I.30)}$$

For each spin up or down magnetic order, the total electron density becomes the sum of the two electron densities

$$\rho(\vec{r}) = \rho_{\uparrow}(\vec{r}) + \rho_{\downarrow}(\vec{r}) \qquad \textbf{(I.31)}$$

The Kohn-Sham equation for the two spins in the form [3]:

$$\begin{cases} \left(\frac{-\hbar^2}{2m}\nabla^2 + V_{eff}^{\uparrow}(\vec{r})\right)\varphi_i(\vec{r}) = \varepsilon_{KS}^{\uparrow}\varphi_i(\vec{r}) \\ \left(\frac{-\hbar^2}{2m}\nabla^2 + V_{eff}^{\downarrow}(\vec{r})\right)\varphi_i(\vec{r}) = \varepsilon_{KS}^{\downarrow}\varphi_i(\vec{r}) \end{cases} \qquad \textbf{(I.32)}$$

The effective potential for the two spins is written as [3]:

$$\begin{cases} V_{\text{eff}}^{\uparrow}(\vec{r}) = V_{\text{ext}} + V_{\text{xc}}^{\uparrow} = V_{\text{ext}} + \dfrac{d\varepsilon_{XC}^{LSDA}[\rho_{\uparrow}(\vec{r}),\rho_{\downarrow}(\vec{r})]}{d\rho_{\uparrow}(\vec{r})} \\ V_{\text{eff}}^{\downarrow}(\vec{r}) = V_{\text{ext}} + V_{\text{xc}}^{\downarrow} = V_{\text{ext}} + \dfrac{d\varepsilon_{XC}^{LSDA}[\rho_{\uparrow}(\vec{r}),\rho_{\downarrow}(\vec{r})]}{d\rho_{\downarrow}(\vec{r})} \end{cases} \qquad \textbf{(I.33)}$$

5.2. The generalized gradient approximation GGA

The previous approximation considered the electron density to be uniformly distributed, making its density homogeneous, but this approximation produced results that were inconsistent with the experimental results on several times, so a new approximation was developed, in which the localized electron density was considered to be non-homogeneous and varied from place to place. Thus, the total energy of the electron system is proportional to both the electron density $\rho(\vec{r})$ and its gradient $\nabla\rho(\vec{r})$, as shown by the equation [25]:

$$E_{XC}^{GGA}[\rho(\vec{r})] = \int d^3\vec{r}\rho(\vec{r})\varepsilon_{XC}[\rho(\vec{r}), \nabla\rho(\vec{r})] \quad \textbf{(I.34)}$$

6. Full-potential linearized augmented plane-wave method (FP-LAPW)

After solving the exchange-correlation potential problem, the search for wave functions as solutions to the Kohn-Sham equation became necessary. After extensive research, certain approaches emerged, including the OPW method presented by Herring theory in 1940 [26], the LMTO method [27], and the FP-LAPW method, where these methods are dependent on the quality of the effective potential utilized.

6.1. The plane wave method (APW)

This method was carried out by the scientist Slater [10] who divided the crystal space into two parts based on the Muffin-Tin approximation [28] (see Figure I.2) by representing the atoms as non-overlapping spheres of radius R_0 in which the core electrons are located, and between these spheres, an interstitial region containing free electrons that are away from the nuclei of their atoms.

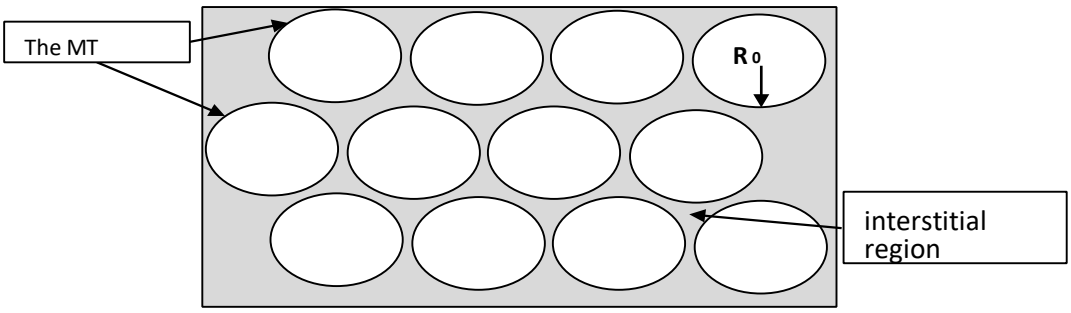

Figure I. 2: Diagram of the distribution of the elementary cell in atomic spheres and in interstitial region.

According to Slater's approximation [10], the core electrons located inside the sphere are subjected to the spherical potential, on the other hand, in the interstitial region the potential is constant [3]. So, the potential in the two regions is given in the form:

$$V(\vec{r}) = \begin{cases} V(r) r \leq R_0 \\ 0 r > R_0 \end{cases}$$

Also, the waves that describe the behavior of electrons inside MT spheres differ from those in the interstitial region, they are described by plane waves in the interstitial region, while inside spheres by functions radials multiplied by spherical harmonics[3]. The two different wave functions are given by the following expression:

$$\varphi(\vec{r}) = \begin{cases} \sum_{l=0}^{\infty} \sum_{-m}^{m} A_{lm} U_l(r) Y_{lm}(r) & r \leq R_0 \\ \frac{1}{\sqrt{\Omega}} \sum_{G} C_G \, e^{i(\vec{K}+\vec{G})\vec{r}} & r > R_0 \end{cases} \quad \textbf{(I.35)}$$

Where Ω: The cell volume

Y_{lm}: Spherical harmonics

A_{lm}: Development coefficients

U_l : The regular solution of the Schrödinger equation given by[29] :

$$\left(\frac{-d^2}{dr^2} + \frac{l(l+1)}{r^2} V(\vec{r}) \right) r U_l = E_l U_l \quad \textbf{(I.36)}$$

Where E_l: An energy parameter.

6.2. The linearized augmented plane wave method (LAPW)

The downside of using the APW method is its slow process in calculations due to the common radial function U_l ; additionally, it is difficult to define the radial function for each

value of energy E_l. So that, Anderson [30] made improvements to the APW method [31]by using the Taylor expansion to write the radial functions U_l (r) in the following form:

$$U_l(r,E) = U_l(r,E_l) + (E_l - E)\frac{dU_l(r,E)}{dE}\Big|_{E=E_l} + O(E_l - E)^2 \quad \textbf{(I.37)}$$

Where the term $\mathcal{O}(E - E_l)^{\,2}$ represents the quadratic error.

After several simplifications, he has got the expression of potential inside and outside of Muffin-Tin balls as follows:

$$V(r) = \begin{cases} \sum_{lm}^{m} V_{lm}(r)Y_{lm} & r \le R_0 \\ \sum_{lm}^{m} V_k(r)e^{ikr} & r > R_0 \end{cases} \quad \textbf{(I.38)}$$

As well as the wave functions inside the spheres in terms of radial functions and their derivatives.{Citation} Where the wave functions are written as follows [32,33]:

$$\Phi_{\vec{K}+\vec{G}}(\vec{r}) = \begin{cases} \sum_{lm} \left(A_{lm}U_l(r) + B_{lm}\dot{U}_l(r)\right)Y_{lm}(r) & r \le R_0 \\ \frac{1}{\sqrt{\Omega}}\sum_{G} C_G\, e^{i(\vec{K}+\vec{G})\vec{r}} & r > R_0 \end{cases} \quad \textbf{(I.39)}$$

Where:

$\vec{K}$: represents the wave vector.

$\vec{G}$: is the vector of the reciprocal lattice.

A_{lm}: are coefficients corresponding to the function U_l.

B_{lm}: are coefficients corresponding to the function U_l.

We can determine the coefficients A_{lm} and B_{lm}, for each wave vector, and for each atom by applying the conditions of continuity of the basic functions in the vicinity of the limit of the spheres. After some simplifications we find the coefficient formula A_{lm} and B_{lm} in the following forms:

$$A_{lm} = \frac{4\pi {r_0}^2 i^L}{\sqrt{\Omega}} {Y^*}_{lm}(K+G) a_l(K+G) \quad \textbf{(I.40)}$$

$$B_{lm} = \frac{4\pi {r_0}^2 i^L}{\sqrt{\Omega}} {Y^*}_{lm}(K+G) b_l(K+G) \quad \textbf{(I.41)}$$

7. WIEN2K simulation code

- ✓ With the technological development, especially programming languages, researchers from the Institute of Materials Chemistry in Vienna were able to design the Wien2k program package [34], which is considered to be one of the most important programs used to study the properties of solid materials. This program consists of many subprograms written in Fortran language, the last of which are algorithms that translate the equations of the crystal system treated according to the density functional theory (DFT) which adopt the method of The full potential linearized augmented plane wave FP-LAPW as a way to compute algorithms to study the properties of compounds[3]. The most important subprograms and its role in the Wien2k code are shown in Figure I.3 which are organized as follows: [3]:
- ✓ **NN** : This subprogram calculates the distances between nearest neighbors up to a specified limit which therefore helps to determine the value of the radius of the atomic sphere.
- ✓ **SGROUP** : determines the space group of the compound.
- ✓ **SYMMETRY** : is a program that defines the symmetry number and space group symmetry operations of our structure.
- ✓ **LSTART** : calculates electron densities in free atoms and show how different orbitals will be treated in band structure calculations.
- ✓ **KGEN** : generates a mesh of K points in the irreducible part of the first Brillouin zone (B.Z). We specify the number of K points in the whole 1stB.Z.
- ✓ **DSTART** : produces an initial density for the SCF cycle (self-consistent cycle) by a superposition of atomic densities produced in the LSTART subprogram.

After the last subprogram ; we enter a loop of SFC calculations and therefore we shall reach five steps :

- ✓ **LAPW0 (POTENTIAL)** : uses the total electron density to calculate the coulomb and exchange potential (Hartree-Fock potential). In addition to that, it divides the space into a MT (muffin-tin) sphere and an interstitial region.
- ✓ **LAPW1 (BANDS) :** calculate eigenvalues and wave functions for valence electrons from solving the equation (III.1).
- ✓ **LAPW2 (RHO)** : calculate the valence electron densities obtained in the step LAPW0.
- ✓ **LCORE** : calculates eigenvalues and wave functions to obtain core electron densities.
- ✓ **MIXER** : calculate the new density by mixing.

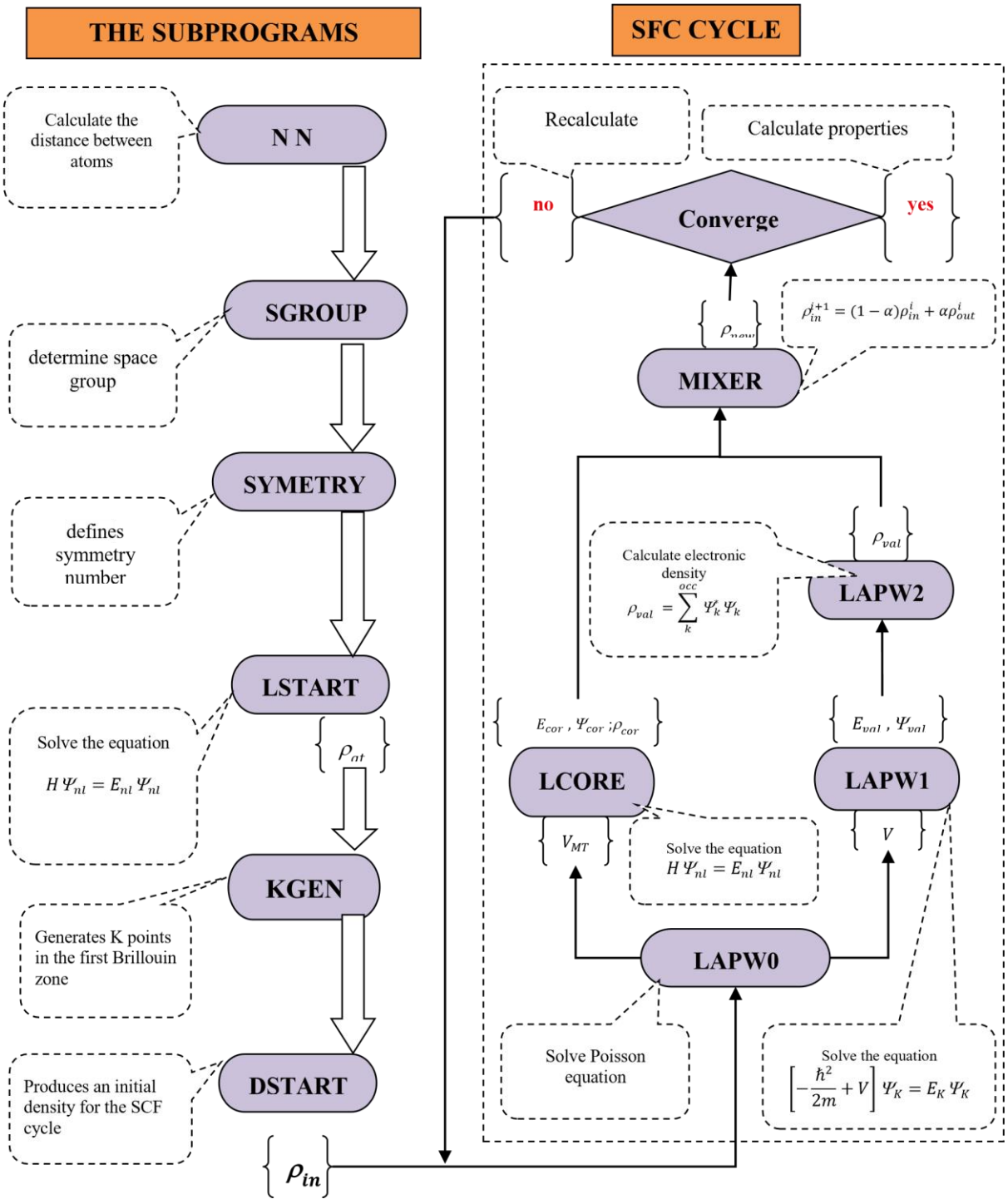

Figure I. 3 : Programs incorporated in Wien2k code [3]

8. References

[1] E. SCHROEDINGER, Quantization as a Problem of Proper Values (Part I), Ann. Phys. (1926). https://ci.nii.ac.jp/naid/10022177951/en/.

[2] S.S. Essaoud, M. Imadalou, D.E. Medjadi, Microscopic Study of Correlations in Finite Fermionic Systems by Breaking the Axial Symmetry, Int J Mod. Theo Phys. 5 (2016) 8–21.

[3] S. Saad Essaoud, Les composés à base de manganèse: investigation théorique des propriétés structurales électroniques et magnétiques, 2020. https://doi.org/10.13140/RG.2.2.30742.68169.

[4] S. Saad Essaoud, Etude microscopique des corrélations dans les systèmes fermioniques finis en brisant la symétrie axiale, 2013. https://doi.org/10.13140/RG.2.2.19283.71203.

[5] M. Born, R. Oppenheimer, Zur Quantentheorie der Molekeln, Ann. Phys. 389 (1927) 457–484. https://doi.org/10.1002/andp.19273892002.

[6] D.R. Hartree, The wave mechanics of an atom with a non-coulomb central field. Part II. Some results and discussion, in: Math. Proc. Camb. Philos. Soc., Cambridge University Press, 1928: pp. 111–132.

[7] D.R. Hartree, The wave mechanics of an atom with a non-coulomb central field. part iii. term values and intensities in series in optical spectra, in: Math. Proc. Camb. Philos. Soc., Cambridge University Press, 1928: pp. 426–437.

[8] G. Shadmon, I. Kelson, Multi-determinantal hartree-fock theory, Nucl. Phys. A. 241 (1975) 407–428. https://doi.org/10.1016/0375-9474(75)90395-4.

[9] V. Fock, „Selfconsistent field “mit Austausch für Natrium, Z. Für Phys. 62 (1930) 795–805.

[10] J.C. Slater, Damped Electron Waves in Crystals, Phys. Rev. 51 (1937) 840–846. https://doi.org/10.1103/physrev.51.840.

[11] P.A.M. Dirac, Note on Exchange Phenomena in the Thomas Atom, Math. Proc. Camb. Philos. Soc. 26 (1930) 376–385. https://doi.org/10.1017/S0305004100016108.

[12] J.C. Slater, A Simplification of the Hartree-Fock Method, Phys. Rev. 81 (1951) 385– 390. https://doi.org/10.1103/PhysRev.81.385.

[13] P. Hohenberg, W. Kohn, Inhomogeneous Electron Gas, Phys. Rev. 136 (1964) B864–B871. https://doi.org/10.1103/physrev.136.b864.

[14] L.H. Thomas, The calculation of atomic fields, Math. Proc. Camb. Philos. Soc. 23 (1927) 542. https://doi.org/10.1017/s0305004100011683.

[15] E. Fermi, Eine statistische Methode zur Bestimmung einiger Eigenschaften des Atoms und ihre Anwendung auf die Theorie des periodischen Systems der Elemente, Z. Für Phys. 48 (1928) 73–79.

[16] Master Thesis, for the compound CsVO3. Marwa, study of electrothermal and thermodynamic properties UNIVERSITE MOHAMED BOUDIAF-M'SILA, 2021.

[17] AgMgF k3MgF, Master AA. Qureshi, a theoretical study of the structural, electronic and optical properties of the two compounds
Thesis, UNIVERSITE MOHAMED BOUDIAF-M'SILA, 2021.

[18] R.M. Dreizler, E.K.U. Gross, Density Functional Theory, (1990). https://doi.org/10.1007/978-3-642-86105-5.

[19] R. Stowasser, R. Hoffmann, What do the Kohn- Sham orbitals and eigenvalues mean?, J. Am. Chem. Soc. 121 (1999) 3414–3420.

[20] A. Seidl, A. Görling, P. Vogl, J.A. Majewski, M. Levy, Generalized Kohn-Sham schemes and the band-gap problem, Phys. Rev. B. 53 (1996) 3764.

[21] C. Fiolhais, F. Nogueira, M.A. Marques, A primer in density functional theory, Springer Science & Business Media, 2003.

[22] F.M. Bickelhaupt, E.J. Baerends, Kohn-Sham density functional theory: predicting and understanding chemistry, Rev. Comput. Chem. 15 (2000) 1–86.

[23] J.A. Pople, P.M. Gill, B.G. Johnson, Kohn—Sham density-functional theory within a finite basis set, Chem. Phys. Lett. 199 (1992) 557–560.

[24] W. Kohn, L.J. Sham, Self-Consistent Equations Including Exchange and Correlation Effects, Phys. Rev. 140 (1965) A1133–A1138. https://doi.org/10.1103/physrev.140.a1133.

[25] D.M. Ceperley, B.J. Alder, Ground State of the Electron Gas by a Stochastic Method, Phys. Rev. Lett. 45 (1980) 566–569. https://doi.org/10.1103/physrevlett.45.566.

[26] C. Herring, A new method for calculating wave functions in crystals, Phys. Rev. 57 (1940) 1169.

[27] H.L. Skriver, The LMTO Method: Muffin-Tin Orbitals and Electronic Structure, Springer-Verlag, Berlin Heidelberg, 1984. https://doi.org/10.1007/978-3-642-81844-8. [28] O.K. Andersen, T. Saha-Dasgupta, Muffin-tin orbitals of arbitrary order, Phys. Rev. B.
62 (2000) R16219.

[29] D D Koelling and G O Arbman, Use of energy derivative of the radial solution in an augmented plane wave method: application to copper, J. Phys. F Met. Phys. 5 (1975) 2041.

[30] O.K. Andersen, Linear methods in band theory, Phys. Rev. B. 12 (1975) 3060–3083. https://doi.org/10.1103/physrevb.12.3060.

[31] M. Petersen, F. Wagner, L. Hufnagel, M. Scheffler, P. Blaha, K. Schwarz, Improving the efficiency of FP-LAPW calculations, Comput. Phys. Commun. 126 (2000) 294–309.

[32] D.R. Hamann, Semiconductor Charge Densities with Hard-Core and Soft-Core Pseudopotentials, Phys. Rev. Lett. 42 (1979) 662–665.
https://doi.org/10.1103/physrevlett.42.662.

[33] M. Weinert, Solution of Poisson's equation: Beyond Ewald_type methods, J. Math. Phys.
22 (1981) 2433–2439. https://doi.org/10.1063/1.524800.

[34] P. Blaha, K. Schwarz, G. Madsen, D. Kvasnicka, J. Luitz, Wien2k, (2001).

Chapter II

Chapter 2 : Results and discussion

Table of Contents

CHAPTER II

Results and Discussions

Summary

The aim of this chapter is to provide a detailed of our computational study of the structural and optoelectronic properties of $BrCdO_2$ *compound, within the TB-mBJ approximation. We also compared all obtained results with other results of experimental and theoretical studies available in previously published works.*

II 1. Introduction

The current state of materials research Delafossite semiconductors has been examined in this chapter, suggesting that this is a key area for continuing and future study. Therefore, we have studied and calculated the linear structural, electronic and optical properties at equilibrium of $BrCdO_2$ compound.

II 2. Simulation details

In this work, the WIEN2k code[1] is used to predict the structural, optoelectronic, of $BrCdO_2$ using the Full Potential-Linearized Augmented Plane Wave (FP-LAPW) approach based on density functional theory (DFT).

For structural properties we used the revised Perdew-Burke-Ernzerhof (PBESol) parameterization of the generalized gradient approximation (GGA)[2], whereas for optoelectronic properties, we used the modified Becke-Johnson exchange potential

(TB-mBJ)[3].

The initialization is presented under a series of programs which generate input files in order to define a starting density, for the determination of the potential and thus the resolution of the Schrödinger equation which gives the eigenvalues and the functions clean. As a result, a new density is generated from the calculated eigenfunctions. This cycle is repeated until convergence is reached.

Before embarking on long and expensive calculations, it is necessary to optimize the input parameters that control the initial calculation density. In general, there are two adjustments to be made:

1- The size of the base of plane waves by the choice of the cutoff Ec (Cutoff Energy) which allows a correct approximation of the eigenfunctions.

2- The quality of the sampling of the Brillouin zone (by the number of kpoints).

The unit cell is separated into muffin-tin spheres that do not overlap and an interstitial area. Wave functions are enlarged in terms of plane waves in the interstitial area, with a cut-off of RMT*KMAX = 8, where RMT is the minimum muffin-tin radius and KMAX is the amplitude of the maximum K vector wave in the Brillouin zone. The optimal value of the cut-off parameter RMT*Kmax was chosen with the help of a convergence test where we calculated

the total energy of the crystalline for different values of RMT*kmax (between 5 and 9), then we plotted the curve of the variation of total energy as a function of RMT*kmax, and we observed that The convergence condition is satisfied from the value of RMT*Kmax = 8 (The difference between the two values of the total energy for both states of RMT*Kmax = 8 and 9 is less than the value of the convergence condition).

Whereas, a spherical harmonic expansion has used inside the spheres with an angular momentum up to l_{max} = 10. The chosen values of the muffin-tin radius R_{MT} for Br, Cd, O_2 atoms are 1.9, 2.1 and 1.6 (a.u) respectively. For the Brillouin zone (BZ) integration, 110 special k-points have been used for $BrCdO_2$, the electronic configurations for valence electrons are for Br ($3d^{10}\ 4s^2\ 4p^5$), Cd ($4d^{10}\ 5s^2$) and O($2s^2\ 2p^4$).To separate between the valence and core states -6 eV was used as separating energy. Both energy (10^{-5} Ry) and charge (10^{-3} e) values were used as criteria for convergence during the calculation.

II 3. Structural properties

Ternary Delafossite with can be crystallized in several types of structures, which directly affect many properties, especially electronic and optical. For this reason, we studied $BrCdO_2$.

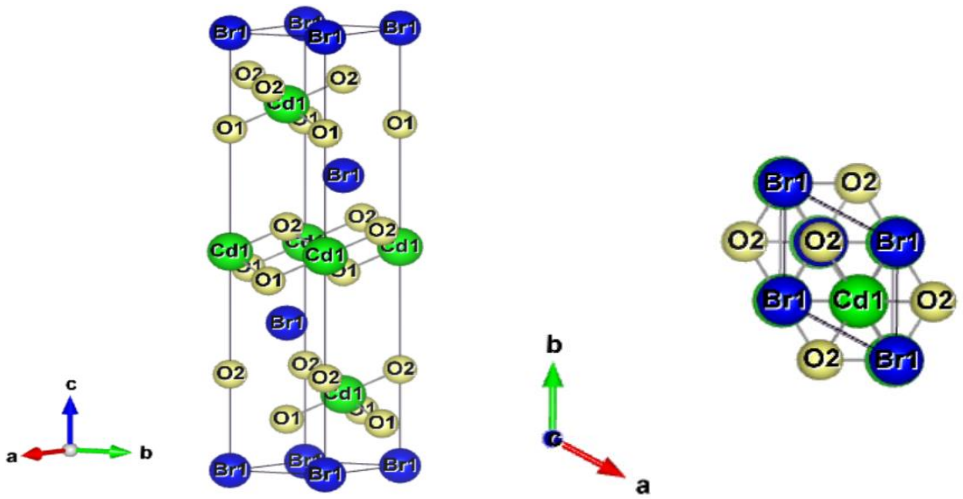

(a) **(b)**

Figure II.1. Crystal structure of $BrCdO_2$ (a) and (b).

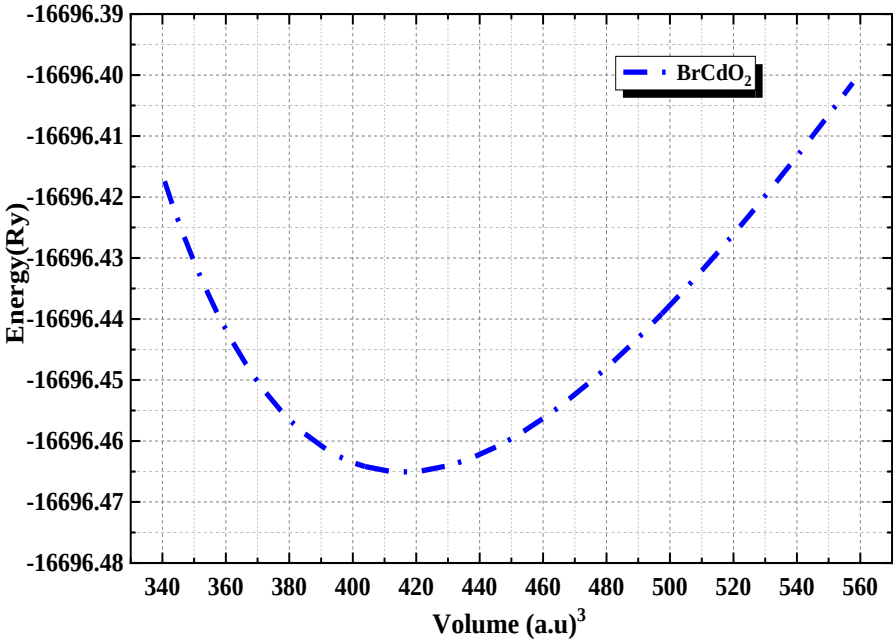

Figure.II.1. Changes in the total energy of the compound $BrCdO_2$ as a function of changes in the volume of the crystal cell.

Before calculating lattice constants, bulk modulus and the cohesive energy, we should determine the atoms positions formed these compound, through full geometry optimizations, the internal atomic positions are relaxed by using the total energy and force minimization scheme basing on Broyden's method [4,5] in which a good relaxed structure can be achieved if the force applied to each atom was smaller than 0.5 Ry/au.

The optimized positions of the atoms for each compound by using GGA approximations are presented in Table.1 and compared to other experimental or theoretical results.

Table II.1. The calculated atomic positions using PBE-Sol approximations of $BrCdO_2$.

		GGA			Other works		
Materials	**Atoms**	**x**	**y**	**z**	**x**	**y**	**z**
$BrCdO_2$ (R-3/m # 166)	Br	0,0000	0,0000	0,0000	0.0000	0.0000	0.3919[8]
	Cd	0.5000	0.5000	0.5000	0.0000	0.0000	0.4925[8]
	O	0.7801	0.7801	0.7801	0.0000	0.0000	0.7597[8]
	O	0,2199	0,2199	0,2199	0.0000	0.0000	0.7597[8]

Computing the lattice parameter "a" of each unit cell is performed by calculating the total energy at different volumes, and then, we use the Murnaghan equation of state [6] to determine the equilibrium volume that correspond to the lowest energy (see Fig.2).

$$E(V) = E_0 + \frac{B}{B'(B'-1)}\left[V\left(\frac{V_0}{V}\right)^{B'} - V_0\right] + \frac{B}{B'}(V - V_0) \quad \text{(II.1)}$$

Where E_0, V_0, B *and* B' are respectively: the total energy, the volume at equilibrium, and the compressibility modulus and its derivative.

The compressibility modulus is given by:

$$B = -V\frac{\partial P}{\partial V} = V\frac{\partial^2 E}{\partial V^2} \quad \text{(II.2)}$$

The volume at equilibrium is given by the minimum of the curve E (V). The equilibrium lattice constants, bulk modulus, and cohesive energy are calculated and denoted summarized in Table II.2 and compared with the other available results, from this table we can see that the finding lattice parameters obtained using GGA approximation for $BrCdO_2$ compounds are in good agreement with the other experimental results. The bulk modulus *B*(GPa) describes the material's resistance to any deformation caused by applying external hydrostatic pressure. Therefore, the bulk modulus values reveal that the $BrCdO_2$ compound is more resistant against regular external pressure where this distinction is attributed to a disparity in the number of bonds, the strength of these bonds between atoms and the difference in structure type between $BrCdO_2$ and the remaining compounds. We can confirm this result by calculating the cohesive energy of these compounds according to the following formula:

$$E_{coh} \qquad \frac{\left(E_{atom}^{Br} + E_{atom}^{Cd} + 2E_{atom}^{O}\right) - E_{atom}^{BrCdO_2}}{4*(N_{Br}+N_{Cd}+N_O)} \quad \text{(II.3)}$$

Where N_{Br}, N_{Cd} and N_o are the numbers of Br, Cd and O atoms, respectively, in the unit cell of the $BrCdO_2$ compound and E_{atom}^{Br}, E_{atom}^{Cd} and E_{atom}^{o} are isolated atoms energies of the Br, Cd and O atoms, respectively, E_{tot}^{BrCdO2} is the total energy of bulk $BrCdO_2$ compound. Comparing the cohesive energy of these compounds leads to finding that the $BrCdO_2$ is more cohesive because it has higher energy and is, therefore, the most structurally stable.

Table II.2. The calculated equilibrium lattice constants, bulk modulus, and cohesive energy for $BrCdO_2$ compounds obtained by using PBE-SOL approximations.

		a (Å)	c(Å)	B(GPa)	E_{coh} (eV/atom)
$BrCdO_2$	GGA	3. 4183	18.2455	65.7258	2.10
	Other cal [14]	3.5130	18.6458	73.48	-
	Exp [8]	3.0240	18.0960	-	-

II 4. Magnetic properties

4.1 The origin of magnetism

In this part we studied the magnetic properties of the compound, and before that we will recall the origin of magnetism in materials [7–12], and this at three levels:

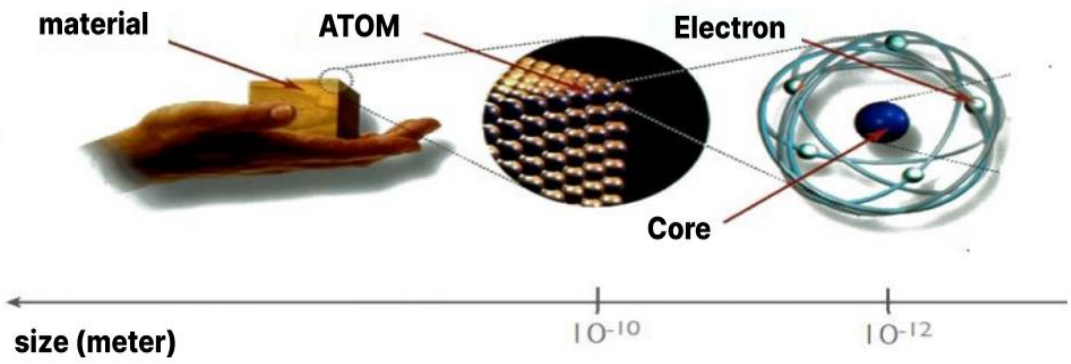

Figure II.2. The origin of magnetism of materials.

4.2 At the electron level :

as we know, each electric charge is in motion, it generates a magnetic field, and since the electron is a particle in motion around itself and around the nucleus , these two movements will generate two magnetic moments:

a) A magnetic moment of spin $\vec{\mu}s = -g\frac{\mu B}{\hbar}\vec{S}$ where g is the Landé parameter and $\hbar$ is the Planck constant.

b) An orbital magnetic moment $\vec{\mu}sI = \frac{\mu B}{\hbar}\vec{I}$ where μB is the Bohr magneton.

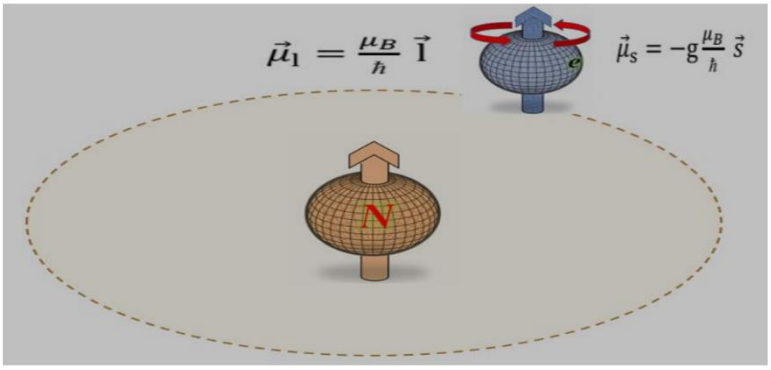

Figure II.3. The origin of magnetism at the electron level

4.3 At the level of the atom :

The magnetism of the atom is linked to the electrons in its outer shell; if all electrons are placed in the outer layer in a paired manner, the sum of the magnetic moments of these two electrons is zero and therefore the atom is non-magnetic, and vice versa.

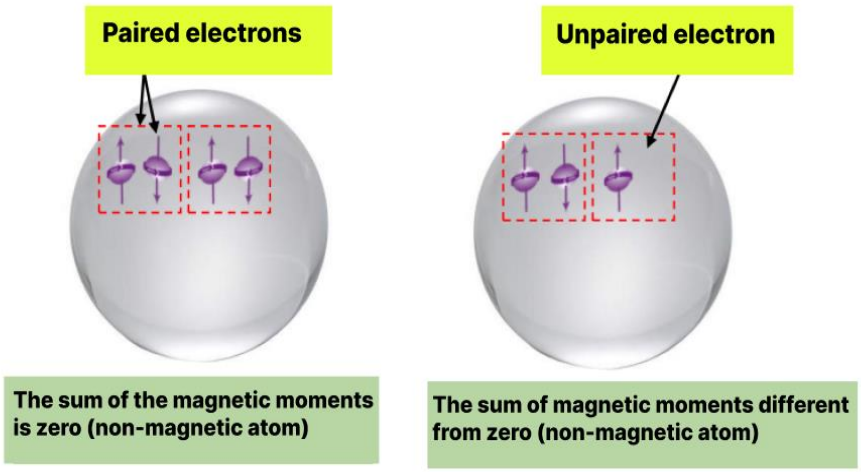

Figure II.4. the origin of magnetism at the atom level.

4.4 At the level of material :

The magnetic state of matter depends on the nature of the atoms making up the matter (magnetic or not), the distances between the atoms and the exchange interactions between them, the effect of temperature and the applied magnetic field. Regarding the magnetic interactions between atoms, they are quantum exchange interactions related to the magnetic moments of the atoms, the distance between them, and the external magnetic field that they are subject to. These interactions were described by the Heisenberg Hamiltonians given by:

$$H_{mag} = \sum_{ij} J_{ij} \vec{S}_i . \vec{S}_j + \sum_i g_i u_B \vec{h} \vec{S}_i \qquad \textbf{(II.4)}$$

Where $\boldsymbol{\mu B}$ is the Bohr magneton, $\boldsymbol{gi}$ is the magnetic ratio, $\vec{\boldsymbol{S}}\,\boldsymbol{i}$ is a spin operator, $\vec{\boldsymbol{h}}$ is the external magnetic field, and $\boldsymbol{Jij}$ is the exchange coupling constant (it depends on the distance between the two atoms). The different states of the magnetic moments of the atoms whose exchange interaction is shown in Figure II.

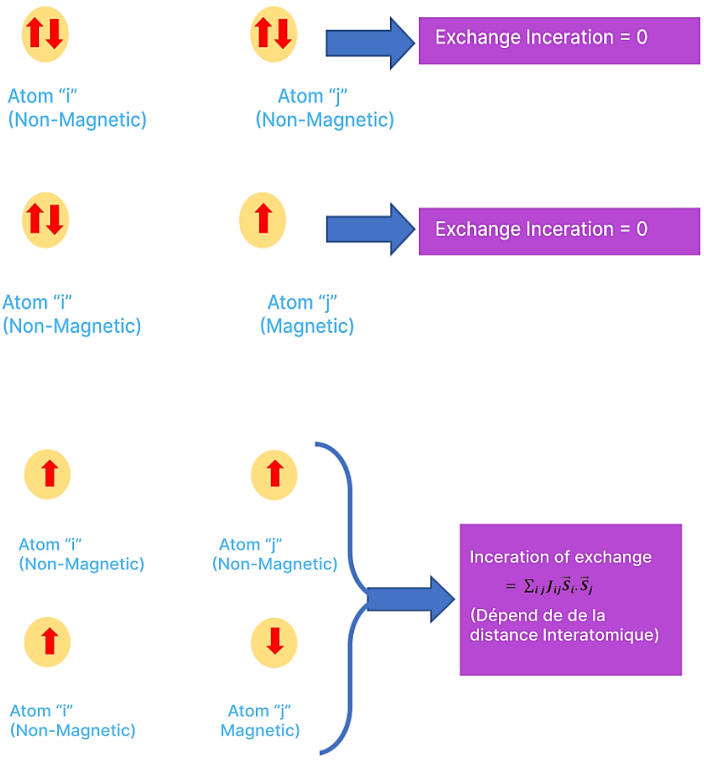

Figure II.5. The origin of magnetism at the level of matter (the different cases of exchange interaction between the magnetic moments of atoms.

Depending on the nature of the atoms making up matter and the alignment of the magnetic moments, we distinguish five types of magnetism:

A) Diamagnetism:

The magnetic material [7–12] consists of non-magnetic atoms, because all its electrons are paired, which means that the total magnetic moment of the atoms is zero.

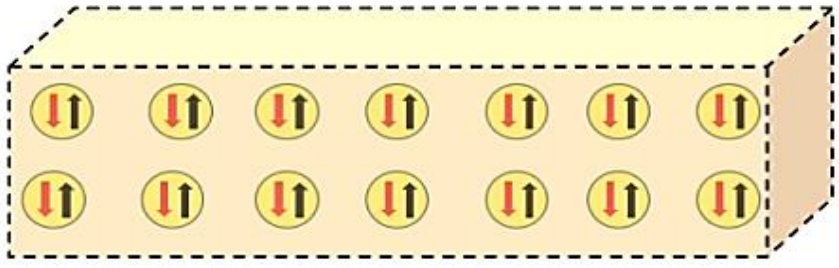

Figure II.6. Illustration of atoms in a state Diamagnetism

B) Paramagnetism:

The atoms of the paramagnetic material contain unpaired electrons, and therefore these atoms have magnetic moments without any exchange interactions between them due to the large distance between them. Therefore its magnetic moments are randomly directed so that the sum of the total torque of the material is equal to zero[7–12].

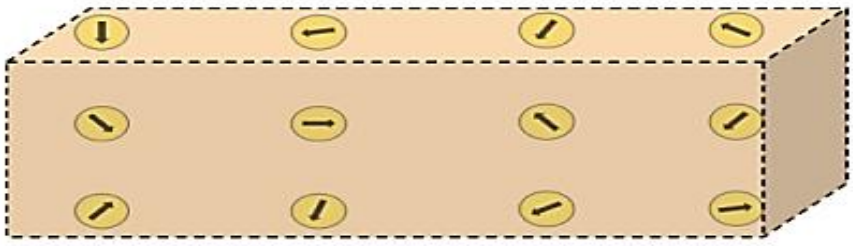

Figure II.7. Illustration of atoms in a state Paramagnetism.

C) Ferromagnetism:

The atoms of the ferromagnetic material are composed of unpaired electrons, an exchange interaction occurs between them due to the small distance between them, so that the exchange integral $\boldsymbol{Jij}$ is negative, so the electrons line up in parallel[7–12].

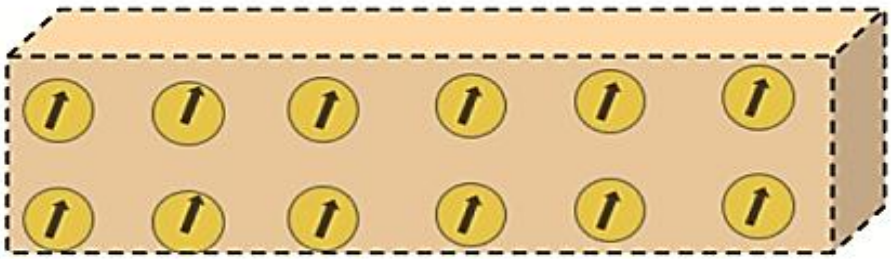

Figure II.8. Illustration of atoms in a state Ferromagnetism.

D) Antiferromagnetism:

The atoms of the antiferromagnetic material are composed of unpaired electrons, an exchange interaction occurs between them due to the small distance is small enough, so the exchange coupling constant $\boldsymbol{Jij}$ is positive , so the electrons align themselves antiparallel, then the atoms are organized in such a way that two neighboring atoms can have opposite magnetic moments and consequently the net moment of the material is zero[7–12].

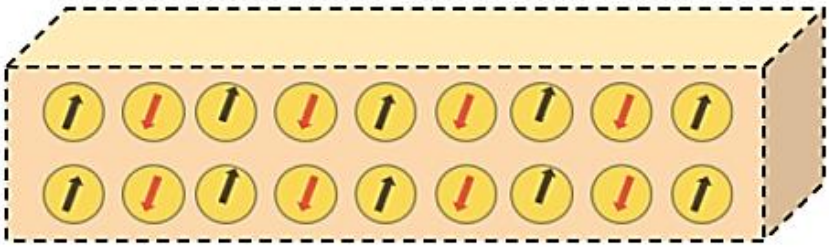

Figure II.9. Illustration of atoms in a state Antiferromagnetism.

E) Ferrimagnetism:

This is a similar state to the antiferromagnetic case, except that the magnetic moments that are arranged antiparallel are not equal, and therefore, the material has a magnetic moment which is not zero [7–12].

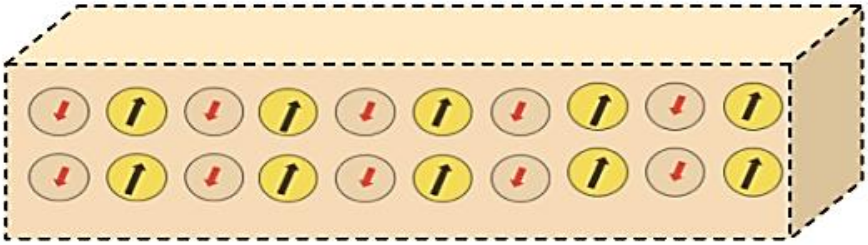

Figure II.10 Illustration of atoms in a state Ferrimagnetism.

4.5 Variation of the magnetic moment under the effect of pressure:

Using the GGA approximation, we were able to calculate the total moment of the maille unitaire as well as the contribution of each atome to this moment. The obtained results, which are shown in Table II.3, indicate that the compound $BrCdO_2$ exhibits ferromagnetic behavior with a total magnetic moment of 3.

It is also observed that the predominant magnetic contributors at this time are the bromum atomes, with the remaining atomes contributing almost nothing.

The variation in the maille's volume can have an impact on the total magnetic moment. As we can see in figure II.11, the magnetic moment increases as the bulk volume of the $BrCdO_2$ compound decreases.

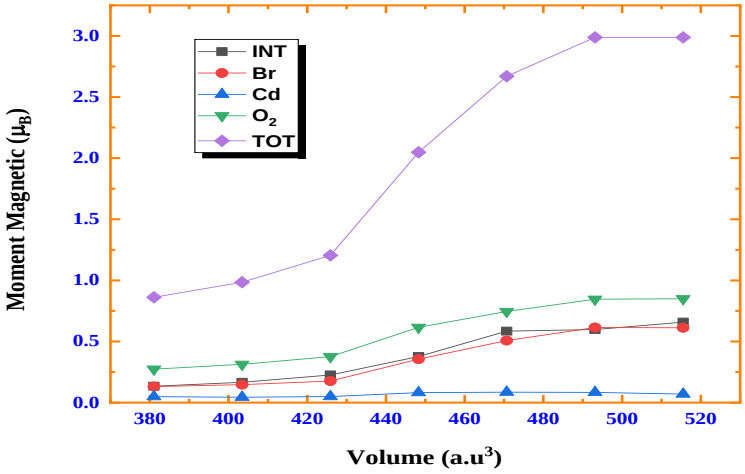

Figure II.11. Total and partial magnetic moment variations as function of volume for $BrCdO_2$.

Table II.3. The entire and partial magnetic moment of $BrCdO_2$.

VOL	INT	Br	Cd	O	TOT
381,0438	0,13436	0,13134	0,04906	0,27364	0,86205
403,458	0,16626	0,1467	0,04454	0,31356	0,98462
425,8724	0,22588	0,17668	0,04963	0,37625	1,2047
448,286	0,37708	0,35584	0,08156	0,61656	2,0476
470,701	0,58509	0,50767	0,08572	0,74548	2,66944
493,1154	0,59814	0,61467	0,08369	0,84572	2,98794
515,5298	0,6584	0,61279	0,06958	0,84997	2,98814

II 5. Electronic properties:

The study of electronic properties is of great importance, as through it we can choose the most appropriate electrical or electronic field for using a material. This purpose is achiev

after knowing the electronic properties of the compound. Therefore, we studied the energy ranges of the two compounds in order to determine the electronic behavior, i.e. to which class of materials it belongs. The studied compound is an insulator, a conductor or a semiconductor) and state density to determine the orbits of atoms that have an effect on each range and thus understand how interatomic bonds are formed.

5.1 BAND STRUCTURE:

Periodically arranged solid systems have discrete energy levels occupied by electrons. These discrete energy levels are hybridized by reciprocal interactions between atoms, splitting them into sub-levels next to one another and producing a continuous energy spectrum called a "energy band." In the most stable state located in the first Brillouin zone, the band structure of $BrCdO_2$ (X = Br, Cd, O_2) compounds has been studied along high symmetry directions. The band structure of $BrCdO_2$ (X = Br, Cd, O_2) in its most stable form is depicted in Figure II.12. It was calculated using the TB-mBJ approximation for the two spin directions, "up" and "down". These figure show that for every chemical under study, the valence and conduction bands overlap in both spin directions.Thus, The development of the band structure in the ferromagnetic state thus displays metallic characteristics in the case of both majority and minority spins.

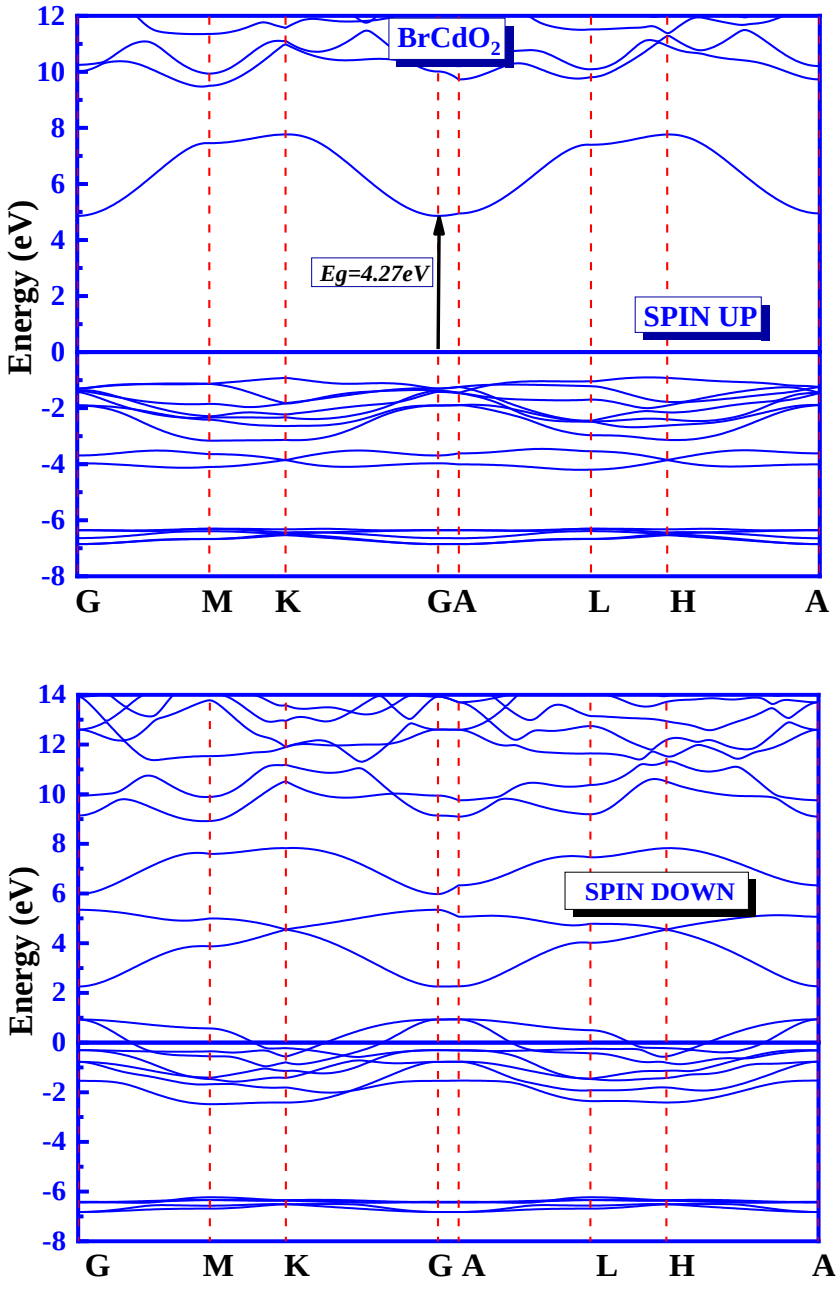

Figure II.12. Calculated band structure for $BrCdO_2$ (Z = Br, Cd and O) within the TB-mBJ approximation.

5.2 ELECTRONIC STATE DENSITY

In solid-state physics, the density of states (DOS) of a system describes the number of electronic states with a given energy. Unlike isolated systems, such as atoms or molecules in the gas phase, density distributions are not discrete like spectral density but continuous. A high DOS at a specific energy level means that many states having that energy and a DOS of zero means that at that energy level no states can be found. We can also use the DOS parameter as

a complementary tool to interpret the formation of certain band structures, and to know the type of hybridization and the states responsible for the binding, so we are talking about the density of total and partial states.

For energies in the interval ε + dε, the density of states (DOS) is defined such that $g(\varepsilon)d\varepsilon$ is the number of energy states in the given range per unit volume, then the DOS is given by a sum over all states with the energy in the interval [ε, ε + dε]. However, since the wave vector k is used to characterize the energy states, we need to add up the total number of states having energy in the interval of interest. By taking into account the spin 2 degeneration factor and normalizing by the volume Ω of the solid, the density of states (DOS) is given by the following expression [13].

$$g(\varepsilon)d\varepsilon = \frac{1}{\Omega}\sum_{k,\varepsilon_k \in [\varepsilon,\varepsilon+d\varepsilon]} 2 = \frac{2}{(2\pi)^3}\int_{\varepsilon_k \in [\varepsilon,\varepsilon+d\varepsilon]} dk \qquad \text{(II.5)}$$

Since the energy in the free electron model does not depend on the angular orientation of the wave vector, i.e.

$$\varepsilon_k = \frac{\hbar^2|k|^2}{2m_e} \Rightarrow kdk = \frac{2m_e}{\hbar^2}d\varepsilon, k = \left(\frac{2m_e\,\varepsilon}{\hbar^2}\right)^{\frac{1}{2}} \qquad \text{(II.6)}$$

For the energy value $\varepsilon_k \in$ [ε, ε + dε] the last two equations give the density of state in a simple spherical symmetry of the form:

$$g(\varepsilon) = \frac{1}{2\pi^2}\left(\frac{2m_e\,\varepsilon}{\hbar^2}\right)^{\frac{3}{2}}\sqrt{\varepsilon} \qquad \text{(II.7)}$$

In the crystal, we can express the density of states by an explicit relation between the DOS and the band structure εi (k) which can be given by the following formula:

$$g(\varepsilon) = \frac{1}{\Omega}\sum_i 2\sum_k \delta\left(\varepsilon - \varepsilon_{i,k}\right) = \sum_i 2\int \frac{dk}{(2\pi)^3}\,\delta\left(\varepsilon - \varepsilon_{i,k}\right) \qquad \text{(II.8)}$$

The computation of the density of states (DOS) in the spin-polarized case is easy so that by using $\varepsilon_{i,k}^{\sigma}$ instead of $\varepsilon_{i,k}$ and $g^{\sigma}(\varepsilon)$ instead of $g(\varepsilon)$ (by replacing the factor 2 by 1) in equation (IV.8) and at the end, we obtain the DOS for each spin state which is written in the form:

$$g^{\sigma}(\varepsilon) = \frac{1}{\Omega}\sum_i 2\sum_k \delta\left(\varepsilon - \varepsilon_{i,k}^{\sigma}\right) = \sum_i 2\int \frac{dk}{(2\pi)^3}\,\delta\left(\varepsilon - \varepsilon_{i,k}^{\sigma}\right) \qquad \text{(II.9)}$$

We can go further and rewrite the expression for TDOS from equation (III.8) [14]:

$$g(\varepsilon) = \frac{1}{\Omega} \sum_i 2 \sum_k \langle \varphi_{i,k} | \varphi_{i,k} \rangle \, \delta \left(\varepsilon - \varepsilon_{i,k} \right) \quad \text{(II.10)}$$

Where $|\varphi_{i,k}\rangle$ are the eigenstates of KS corresponding to the eigenvalues $\varepsilon_{i,k}$.

We can calculate the partial (projected) density of states (PDOS) $n_i\ (\varepsilon)$ after calculating the polarized spin, we choose to project the TDOS on the atomic orbitals (e.g., s, p and d) to get the contribution partial of each atomic orbital [13]:

$$n_i\ (\varepsilon) = \sum_n \delta\ (\varepsilon - \varepsilon_n) |P_{ni}^a|^2 \quad \text{(II.11)}$$

To understand the formation of each band in band structure spectra, we analyze the total and the partial density of the atomic orbitals states that shown in Figure II.3. According to this figure, we notice that there is no density of the state around the Fermi level, which confirms the semiconductor behavior of these compounds. Also, for $BrCdO_2$ in its Tetragonal phase structure, it is clear that the conduction band is formed mainly by the dominant contribution of the "d" orbitals of the cadmium atom, with the presence of weak contribution from "p" orbitals of Br and O in the range of -5 eV to 0 eV, in addition a very weak contribution from the electrons of the "p" orbital of the "O" atom and "s" of the Cd atom.

For the conduction band, the partial density curves for both $BrCdO_2$ appears a dominant contribution of "d" orbital of Cd atoms. Through total partial density of states analysis, our obtained results are similar to the previous studies [13,15].

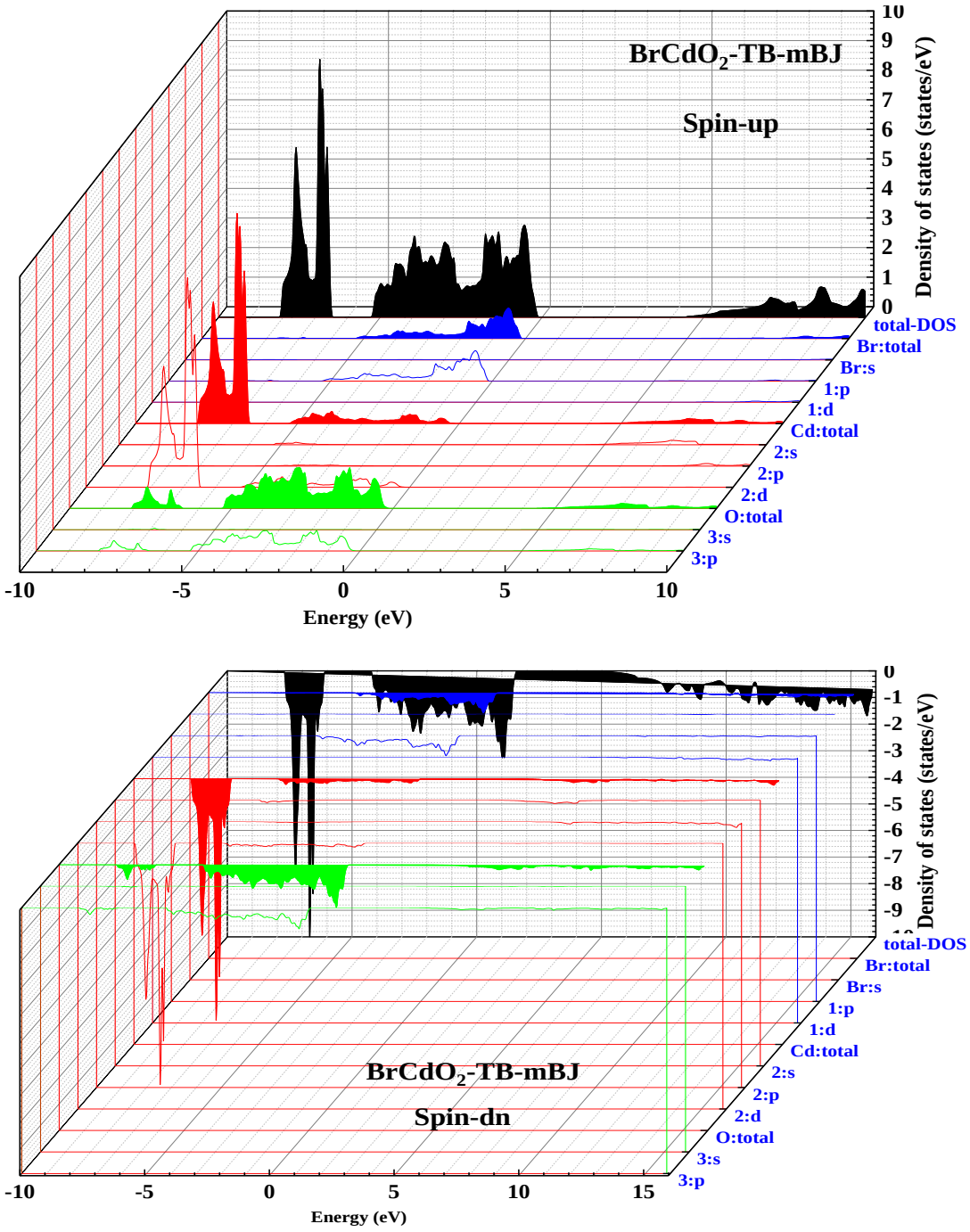

Figure II.13. Calculated total and partial density of states for $BrCdO_2$ within the TB-mBJ approximation.

The contributions of the atomic orbitals can be divided with respect to the energy shown in Figure II.13 for compound $BrCdO_2$.

The range [-10 to -5]: is a very strong contribution from the electrons of the "d" orbital of the "Cd" atom.

The range [-5 to 0]: A weak contribution from the electrons of the “p” orbital of the “Br” and “O” atoms.

The range [5 to 10] A very weak contribution from the electrons of the “p” orbital of the “O” atom and “s” of the Cd atom.

II 6. Optical properties :

The way that light interacts with solid materials depends on their electronic properties (i.e., whether they are semiconductors, insulators, or conductors), electronic density, the distance separating valence bands from conduction, the number of bonding between atoms, and whether they are ionic or covalent. More specifically, if the solid material is a semiconductor, this difference is mostly caused by the energy that the electromagnetic waves carry and how they interact with valence band electrons and photons as the electromagnetic waves' electric field interacts with the electrons that are polarized in the same direction. The polarization of light allows light to excite the valence electrons, which in turn allows the electrons to shift from the valence band to the conduction band in a process known as the interband transition. This allows light energy to be absorbed. The examination of the electronic density of state allows for the deduction and identification of the electrons involved in the excitation, the energy band in which the interphase transition takes place, and the atomic orbital to which they transition. Light is refracted and its course is altered as a result of polarization, which also causes these electromagnetic waves to travel through materials at a slower pace due to their interaction with the material's electrons [16–19]. As a result, every material interacts with light differently from the others, whether it is in terms of how well it can absorb light, how it can alter light with respect to its refractive index and reflection coefficient, or how quickly light loses some of its energy. Whether used as optical filters, optical detectors, sensors, or anti-reflective coatings, these characteristics can direct and assess a material's suitability for a given application [16–19].

The study of light-matter interaction to deduce the optical behavior of solids is described mathematically through the dielectric function $\varepsilon(\omega)$ which is given in terms of the real part $\varepsilon_1(\omega)$ and the imaginary part $\varepsilon_2(\omega)$ with the following expression [20-23]:

$$\varepsilon(\omega) = \varepsilon_1(\omega) + i\varepsilon_2(\omega) \qquad \text{(II. 12)}$$

The real part (ε_1) of the dielectric function represents the scattering of incident photons by parts of the material [24], which gives us an idea about the state of electronic polarization of the material, while the imaginary part (ε_2) expresses the energy absorbed by the material [25]. The imaginary part (ε_2) is estimated using the structure of the electronic energy bands, that is, by connecting the elements of the moment matrix for the occupied and unoccupied electronic states [26], while the real part (ε_1) can be obtained by relying on the transformation Kramer-Cronje [27].

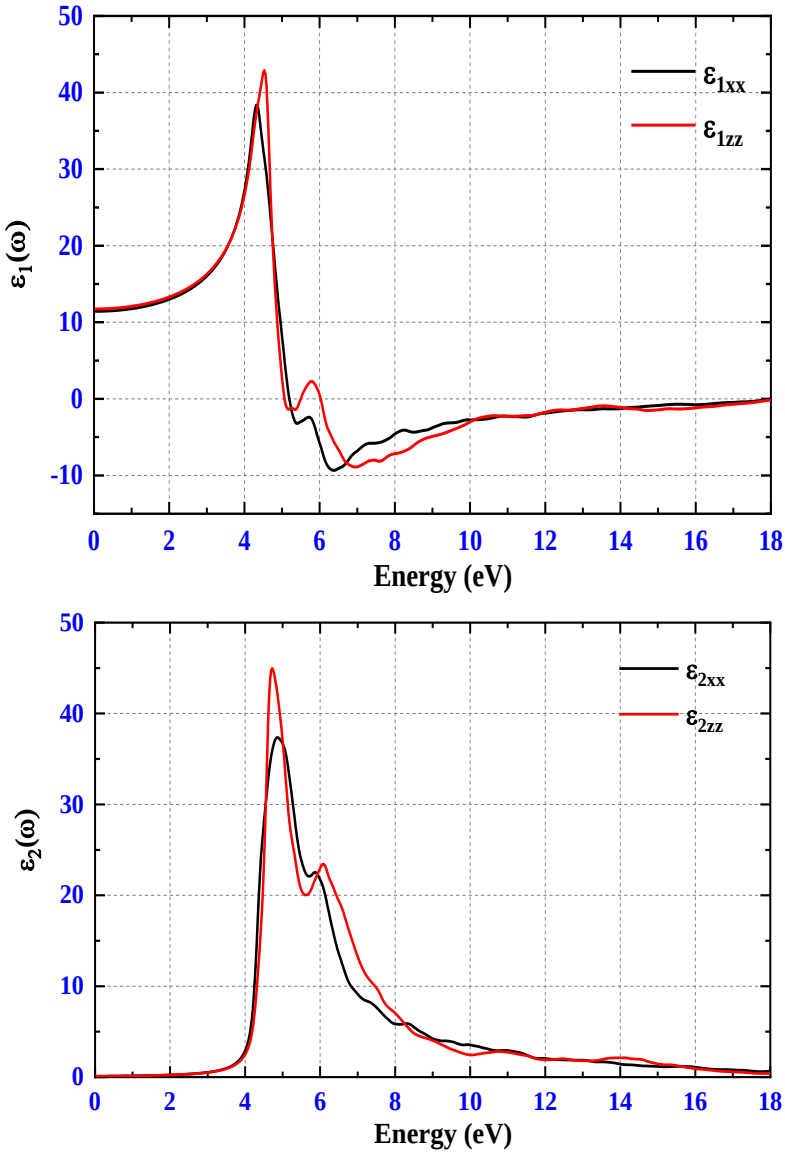

Figure II.14. Real and imaginary part of the dielectric function for $BrCdO_2$ within TB-mBJ approximation compared the real one with other computational work. Regarding the spectra of the imaginary part ε2(ω) plotted in figures (II.14), we can see that the optical band gaps obtained

from the imaginary part of the dielectric function calculated using TB-mBJ approximation are 4.27 eV for $BrCdO_2$. The $\varepsilon_2(\omega)$ spectra express the absorption that can occur as a result of electronic excitation from the valence states below the Fermi level to the conduction states where through this spectra we can observe that this absorption can only occur if the energy value of the incident photons is greater than the energy gap.

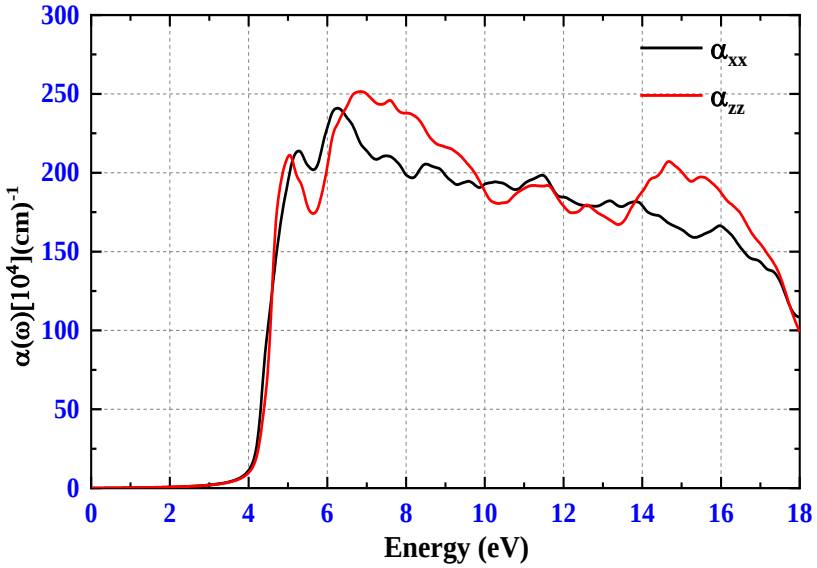

Figure II.15. Absorption coefficient of $BrCdO_2$ within TB-mBJ approach.

According to Figure.II.15, the absorption edge is located at around 4.27 eV for $BrCdO_2$, where all the studied compound have a good response in the range of 5.0 to 18eV for $BrCdO_2$ to incident photons.

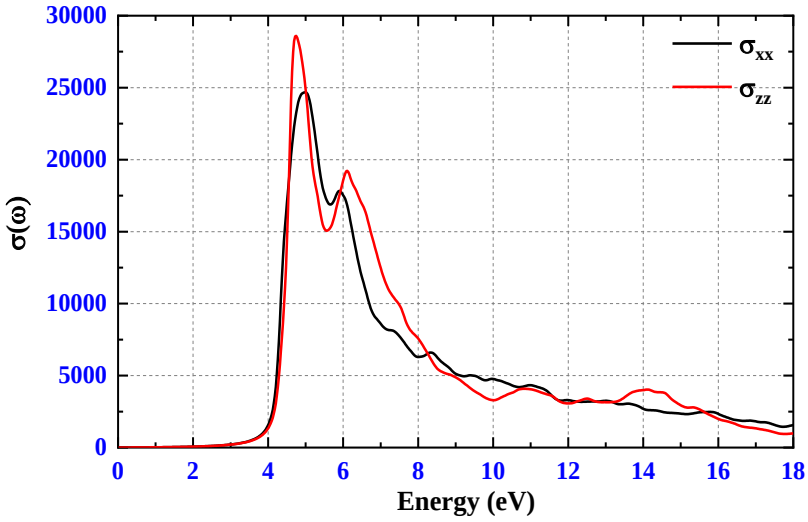

Figure II.16. Optical conductivity of $BrCdO_2$ using TB-mBJ approach.

Optical conductivity is a complex quantity defined by the following formula [28]:

$$\sigma(\omega) = -\frac{i\omega}{4\pi}\varepsilon(\omega) \qquad \text{(II.13)}$$

Figure II.16 shows that the optical conductivity starting from 2.8 eV to $BrCdO_2$. As remark, the maximum of optical conductivity of the compounds is at 5.1 eV.

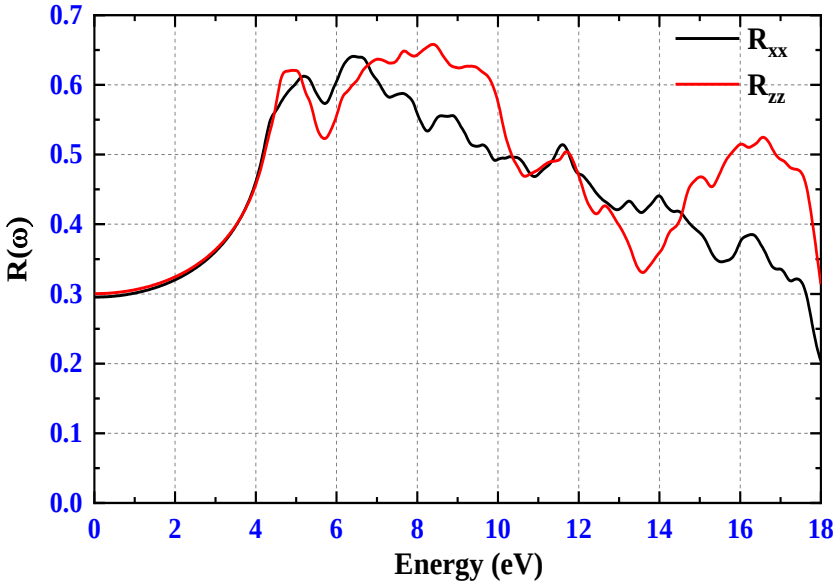

Figure II.17. Optical reflectivity of $BrCdO_2$ using TB-mBJ approach.

We define another parameter, which is the reflectivity coefficient R(ω). This parameter characterizes the part of the reflected energy from the solid surface and can be derived by the refractive index [29] as follows :

$$R(\omega) = \left|\frac{(n(\omega)-1)^2+k^2(\omega)}{(n(\omega)+1)^2+k^2(\omega)}\right| \qquad \text{(II.14)}$$

The optical reflectivity of $BrCdO_2$ was displayed as a function of light energy in Figure II.17. It was discovered that $BrCdO_2$ zero-frequency reflectivity limit is 0.3. It is also evident that the high reflectivity peaks is found at energie of 6.4

8 Conclusion:

The structural, electrical, magnetic, and optical characteristics of the compound $BrCdO_2$ were theoretically analyzed for this thesis using the Wien2k simulation code and density functional theory ("DFT"), which is based on the full-potential linearized augmented plane wave (FP-LAPW).

The study conducted on the compound provided is an incentive to search for another substance from the same class of compounds studied, and this is after we recorded the following points:

- Study of the compound: The compound crystallizes in structure that has a high level of symmetry, which makes it easy for us to perform calculations in a short time easy for us to perform the calculations in a short time.
- The methods employed to estimate the exchange-correlation potential produced results extremely close to the experimental data, indicating that the experimental and theoretical sides are in excellent accordance.
- The dominant goal through this memorandum has been achieved, which is to add the foundations of quantum mechanics to exploring the properties of materials, and this in the end is to direct and determine the appropriate field for the use of this compound $BrCdO_2$, as well as to know the type of atoms that affect certain properties in order to control them. Factors can also be determined. Which affects these properties and finally predicts other materials or other properties that they may possess if a certain aspect is changed or influenced by an external factor.

From a scientific standpoint, through our study of compound, we concluded the following results:

- The composite's structural qualities make it more cohesive and resistant to outside pressure.
- Regarding the electronic properties, the compound has a semiconductor, as we observed an energy that separates the valence band from the conduction band.
- The substance under investigation has ferromagnetic characteristics.
- We can determine that a compound is magnetic by looking at its magnetic characteristics.
- $BrCdO_2$, with an absorption coefficient is high. They are therefore potential candidates for photovoltaic applications.

9 References :

[1] P. Blaha, K. Schwarz, G.K. Madsen, D. Kvasnicka, J. Luitz, wien2k, Augment. Plane Wave Local Orbitals Program Calc. Cryst. Prop. (2001).

[2] J.P. Perdew, K. Burke, M. Ernzerhof, Generalized gradient approximation made simple, Phys. Rev. Lett. 77 (1996) 3865–3868.

[3] A.D. Becke, E.R. Johnson, A simple effective potential for exchange, American Institute of Physics, 2006.

[4] C.G. Broyden, The convergence of a class of double-rank minimization algorithms: 1. general considerations, IMA J. Appl. Math. 6 (1970) 76–90.

[5] C.G. Broyden, The convergence of a class of double-rank minimization algorithms: 2. The new algorithm, IMA J. Appl. Math. 6 (1970) 222–231.

[6] F.D. Murnaghan, The compressibility of media under extreme pressures, Proc. Natl.Acad. Sci. U.S.A. 30 (1944) 244.

[7] J.C. Slater, Damped Electron Waves in Crystals, Physical Review. 51 (1937) 840–846. https://doi.org/10.1103/physrev.51.840.

[8] P. Kushwaha, H. Borrmann, S. Khim, H. Rosner, P.J.W. Moll, D.A. Sokolov, V. Sunko, Y. Grin, A.P. Mackenzie, Single crystal growth, structure, and electronic properties of metallic delafossite $PdRhO_2$, Cryst. Growth Des. 17 (2017) 4144–4150.

[9] J.C. Slater, A Simplification of the Hartree-Fock Method, Phys. Rev. 81 (1951) 385–390. https://doi.org/10.1103/PhysRev.81.385.

[10] P. Hohenberg, W. Kohn, Inhomogeneous Electron Gas, Physical Review. 136 (1964) B864–B871. https://doi.org/10.1103/physrev.136.b864.

[11] L.H. Thomas, The calculation of atomic fields, Mathematical Proceedings of the Cambridge Philosophical Society. 23 (1927) 542.

[12] E. Fermi, Eine statistische Methode zur Bestimmung einiger Eigenschaften des Atoms und ihre Anwendung auf die Theorie des periodischen Systems der Elemente, Zeitschrift Für Physik. 48 (1928) 73–79.

[13] M.G. Brik, First-principles calculations of the structural, electronic, optical and elastic properties of the $CuYS_2$ semiconductor, J. Phys. Condens. Matter. 25 (2013) 345802.

[14] M.D. Heinemann, F. Ruske, D. Greiner, A.R. Jeong, M. Rusu, B. Rech, R. Schlatmann, C.A. Kaufmann, Advantageous light management in Cu(In, Ga)Se_2 superstrate solar cells, Sol. Energy Mater. Sol. Cells. 150 (2016) 76–81.

[15] J. Jiang, W. Zhou, Y. Xue, H. Ning, X. Liang, W. Zhou, J. Guo, D. Huang, Intermediate band insertion by group-IIIA elements alloying in a low cost solar cell absorber $CuYSe_2$: A first-principles study, Phys. Lett. A. 383 (2019) 1972–1976.

[16] *بري,السعدي* ,X2GdIn (Au,Ag,Cu) *مساهمة في دراسة الخصائص الفيزيائية ل* , X2GdIn (X= Au, Ag, Cu), PhD Thesis, 2019.

[17] F. MEZRAG, Etude des propriétés optoélectroniques et diélectriques des matériaux semiconducteurs, PhD Thesis, Université Mohamed Khider-Biskra, 2012.

[18] F. Mezrag, Effet du désordre compositionnel sur les propriétés optoélectroniques et diélectriques de l'alliage ternaire semiconducteur GaAsxSb1-x, PhD Thesis, Université de M'Sila-Mohamed Boudiaf, n.d.

[19] F. Mezrag, N. Bouarissa, Optical properties of AlxInl-xP ternary semiconductor alloys, J. Comput. Methods Sci. Eng. 18 (2018) 299-305.

[20] M.A. Khan, A. Kashyap, A.K. Solanki, T. Nautiyal, S. Auluck, Interband optical properties of Ni 3 Al, Phys. Rev. B. 48 (1993) 16974.

[21] Optical Properties of Materials and Their Applications, 2nd Edition | Wiley, Wiley.Com. (n.d.).https://www.wiley.com/enus/Optical+Properties+of+Materials+and+Their+Applications%2C+2nd+Edition-p9781119506317 (accessed February 4, 2021).

[22] C. Ambrosch-Draxl, J.O. Sofo, Linear optical properties of solids within the full-potential linearized augmented planewave method, Comput. Phys. Commun. 175 (2006) 1–14.

[23] M. Gajdoš, K. Hummer, G. Kresse, J. Furthmüller, F. Bechstedt, Linear optical properties in the projector-augmented wave methodology, Phys. Rev. B. 73 (2006) 045112.

[24] B.U. Haq, S. AlFaify, A.S. Jbara, R. Ahmed, F.K. Butt, A. Laref, A.R. Chaudhry, Z.A. Shah,Optoelectronic properties of three PbSe polymorphs, Ceram. Int. 46 (2020) 22181-22188.

[25] A.S. Jbara, Z. Othaman, H.A. Aliabad, M.A. Saeed, Electronic and Optical Properties of y- and -Alumina by First Principle Calculations, Adv. Sci. Eng. Med. 9 (2017) 287-293.

[26] A.S. Jbara, J. Munir, B.U. Haq, M.A. Saeed, Density functional theory study of mixed halideinfluence on structures and optoelectronic attributes of CsPb (I/Br) 3, Appl. Opt. 59 (2020) 3751-3759.

[27] H. Tributsch, Solar energy-assisted electrochemical splitting of water. Some energetical, kinetical and catalytical considerations verified on MoS2 layer crystal surfaces, Z. Für Naturforschung A. 32 (1977) 972-985.

[28] C. Ambrosch-Draxl, J.O. Sofo, Linear optical properties of solids within the fullpotential linearized augmented planewave method, Comput. Phys. Commun. 175 (2006) 1–14.

[29] H. Tributsch, Solar energy-assisted electrochemical splitting of water. Some energetical, kinetical and catalytical considerations verified on MoS_2 layer crystal surfaces, Z. Für Naturforschung A. 32 (1977) 972–985.

General Conclusion

General conclusion

Delafossite-type ABO_2 oxides have a bright future and they are consistently findings applications in various sectors. We are putting here few of the challenges which are dealing in current research for a future prospectus. From the synthesis and processing point of view, these materials should have cheap manufacturing process. These materials enlarge an excellent challenge for their function and implementation in sensor devices due to their good sensor-specific advantages. The study conducted on the presented compound highlights the potential for exploring other substances within the same class of compounds.

The study conducted on the presented compound highlights significant potential for exploring other substances within the same class of compounds. Firstly, it was found that the compound crystallizes in structure with a high degree of symmetry, which greatly facilitates quick and efficient computational processes. This structural characteristic simplifies the calculations and enables more accurate predictions of the compound's behavior.

Moreover, the methods used to estimate cross-correlation potentials yielded results that closely matched experimental data. This close alignment between theoretical predictions and experimental observations indicates a robust agreement, enhancing the reliability of the theoretical models used.

The primary objective of the study was to integrate the foundations of quantum mechanics to explore the properties of materials. This goal was successfully achieved, providing valuable insights into the appropriate applications for the compound $BrCdO_2$. The study also identified the types of atoms that influence specific properties, enabling better control over these properties. Furthermore, by understanding the factors that affect these properties, researchers can predict other materials or properties that may arise if certain conditions are altered or influenced by external factors.

From a scientific perspective, the study revealed several important findings. The structural qualities of the compound make it more consistent and resistant to external pressures, highlighting its potential for use in various demanding environments. Additionally, the electronic properties of the compound indicate that it behaves as a semiconductor, with a distinct energy gap separating the valence band from the conduction band. This property is crucial for applications in electronic devices and sensors.

Furthermore, the material under investigation exhibits ferromagnetic properties. By examining these properties, it was possible to determine the compound's magnetic nature, which could be advantageous for applications in magnetic storage and other technologies.

Overall, these findings underscore the importance of further research in this field. The studied compound, along with similar materials, holds promise for diverse applications in electronics, optoelectronics, and magnetic devices. Continued exploration and experimentation could lead to the discovery of new materials with enhanced or novel properties, driving innovation and technological advancement in various sectors.

ملخص

قمنا بدراسة نظرية لحساب الخواص البنيوية، الاكترونية و الضوئية والمغناطيسية لمركب $BrCdO_2$ في إطار نظرية دالية الكثافة (DFT) وباستعمال برنامج Wien2K المعتمد على طريقة االمواج المستوية المتزايدة خطيا(FP_LAPW) وهذا بالاعتماد على كل من تقريب التدرج المعمم (GGA) والتقريب المعدل (mBJ) لحساب كمون تبادل_ارتباط . فيما يخص الخواص البنيوية، حددنا قيم كل من ثابت الشبكة، معامل الانضغاطية وطاقة التماسك. ولفهم السلوك الاكتروني للمركب قمنا بحساب وتحليل بنية عصابات الطاقة الاكترونية وكثافة الحالة الاكترونية الكلية (TDOS) والجزئية .(PDOS) ومن جهة أخرى قمنا أيضا بدراسة الخصائص المغناطيسة والعزم المغناطيسي الكلي والجزئي للذرات المكونة للمركب. في نهاية عملنا قمنا بحساب الخواص الضوئية وهذا بعد حساب الجزء الحقيقي والتخيلي لدالة العزل ومن ثم استخراج بقية المعاملات الضوئية كالامتصاص، معامل الانكسار واالناقلية الضوئية.

summary

We conducted a theoretical study to calculate the structural, electronic, optical and magnetic properties of $BrCdO_2$ within the framework of density function theory (DFT) and using the Wien2K program based on the method of linearly increasing plane waves (FP_LAPW), and this is based on both the generalized gradient approximation (GGA) and the modified approximation (mBJ). To calculate the link exchange latency. Regarding the structural properties, we determined the values of the network constant, compressibility coefficient and cohesion energy. To understand the electronic behavior of the compound, we calculated and analyzed the structure of the electronic energy bands and the total and partial electronic density of state (TDOS). On the other hand, we also studied the magnetic properties and the total and partial magnetic moments of the atoms that make up the compound. Finally, we calculated the optical properties by computing the real and imaginary parts of the dielectric function and subsequently deriving other optical parameters such as absorption, reflectivity coefficient, and optical conductivity..

.